TECHNICAL UNIVERSITY – GABROVO

Faculty of Mechanical and Precision Engineering

Mag.Eng. Krasen Ivanov Kostov

INTELLIGENT CONTROL OF ELECTRO-HYDRAULIC DRIVE SYSTEM

AUTHOR'S SUMMARY

of a dissertation for acquiring the educational and scientific degree "Ph. Doctor"

Field of higher education: 5 "Technical Sciences"

Professional field: 5.1 "Mechanical Engineering"

Doctoral Program: "Hydraulic and Pneumatic Drive Systems"

GABROVO
2026

TECHNICAL UNIVERSITY – GABROVO

Faculty of Mechanical and Precision Engineering

Mag.Eng. Krasen Ivanov Kostov

INTELLIGENT CONTROL OF ELECTRO-HYDRAULIC DRIVE SYSTEM

AUTHOR'S SUMMARY

of a dissertation for acquiring the educational and scientific degree "Ph. Doctor"

Field of higher education: 5 "Technical Sciences"

Professional field: 5.1 "Mechanical Engineering"

Doctoral Program: "Hydraulic and Pneumatic Drive Systems"

Scientific supervisors:

Assoc. Prof. Dr. Eng. Krasimir Hristov Ormandzhiev

Assoc. Prof. Dr. Eng. Stanimir Yordanov Yordanov

GABROVO

2026

The dissertation was discussed and directed for defense by an extended department council from the Department of Power Engineering at the TECHNICAL UNIVERSITY - GABROVO, at a meeting held on ……….

The research for the dissertation was carried out in the Department of Power Engineering,

TU-Gabrovo

The defense of the dissertation will take place on ………………….2026 at …………..time in the hall of TU-Gabrovo at a meeting

The materials for the defense are available to those interested in the office of the department …………………………………

Author: Eng. Krasen Ivanov Kostov

Title: INTELLIGENT CONTROL OF AN ELECTRO-HYDRAULIC DRIVE SYSTEM

Format:

Printed cars:

Circulation:

Printing: University Publishing House "Vasil Aprilov" - Gabrovo

GENERAL CHARACTERISTICS OF THE DISSERTATION

Relevance of the research topic: Modern electro-hydraulic systems for automatic control are widely used in industrial, transport and energy systems, where high accuracy, speed and reliability are required in the presence of significant external influences and internal nonlinearities. A characteristic feature of these systems is their complex dynamics, determined by the joint influence of hydraulic, mechanical and electrical processes, which leads to the presence of nonlinearities, parametric uncertainties and disturbing effects.

In real-world operation, electrohydraulic tracking systems operate under variable load conditions, changes in the parameters of the operating environment, and the presence of external disturbances, which significantly worsens the dynamic characteristics of the system. This is manifested in increased overshoot, extended settling time, oscillatory nature of transients, and reduced stability. As a result, a decrease in the operational reliability and efficiency of the control systems is observed.

Purpose of the dissertation: The main goal of this dissertation is to increase the quality, stability and robustness of the control of an electro-hydraulic tracking system with a rotary actuator by developing and researching adaptive, intelligent and robust control methods that ensure effective operation in the presence of nonlinearities, parametric changes and external disturbances.

Main tasks of the dissertation:

To achieve the formulated goal, the following research tasks have been set:

1. To perform an in-depth theoretical analysis of the dynamic properties of electrohydraulic systems in the presence of nonlinearities, hysteresis effects, and parametric uncertainties.
2. To develop adequate mathematical and simulation models of an electrohydraulic tracking system in the *MATLAB/Simulink* environment, allowing for the study of the system in modes close to real time.
3. To carry out verification and experimental validation of the developed models by conducting laboratory tests under different operating modes.
4. To identify the main parameters of the system based on experimental data, in order to increase the adequacy of the models.
5. To synthesize a classic *PID* controller and to evaluate its dynamic performance and limitations in controlling the electrohydraulic system.
6. To design and analyze Fuzzy *and* adaptive *Fuzzy – PID* controllers and to investigate their effectiveness under variable operating conditions and uncertainties.
7. To synthesize a robust H_∞controller in the presence of structured uncertainties and to analyze its properties in terms of stability and robustness.
8. To conduct a quantitative comparative analysis of different control strategies using quality indicators such as settling time t_s, overshoot σ, static error and integral quality criteria.

The scientific novelty of the dissertation work is expressed in:

- The development and research of a nonlinear and linearized mathematical model of an automated electrohydraulic tracking system with a rotary actuator, taking into account the basic physical processes, dynamic dependencies and nonlinearities of the object.

- The development of a methodology and software implementation for parametric identification of electro-hydraulic tracking systems under different load regimes, ensuring increased adequacy and reliability of the mathematical model in conditions of nonlinearity and uncertainty.
- Synthesis and comparative study of intelligent and robust control methods – *Fuzzy*, adaptive *Fuzzy–PID* and H_∞ controllers, adapted to the specifics of electro-hydraulic systems, as well as the development of an adaptive structure for online tuning of the controller parameters in order to improve dynamic performance and resistance to external disturbances.

Practical applicability

The practical significance of the obtained results is expressed in the development of models, algorithms and management tools applicable to:

- design, research, analysis and tuning of electro-hydraulic tracking systems using the developed hardware-software platform and *MATLAB/Simulink* real-time model;
- modeling and evaluation of the influence of different loading regimes on the dynamic characteristics of electro-hydraulic systems;
- synthesis and implementation of intelligent and robust controllers to increase the accuracy, speed and stability of systems in the presence of disturbances and parametric uncertainties;
- optimization and modernization of existing automatic control systems in industrial, laboratory and research applications.

The developed solutions can be used in the design of new electro-hydraulic systems, as well as in the improvement of existing automatic control systems requiring high dynamic accuracy, reliability and robustness.

Publication of the results of the dissertation research The analyses performed, the developed methodologies and the obtained results for the period from 2020÷2026 are presented in 7 publications related to the work on the topic of the dissertation. One of them is independent , 2 articles are published in refereed journals in Bulgarian. Four of the publications are refereed in Scopus, one of them has SJR = 0.203. 4 citations have been registered in Scopus.

Structure and scope of the dissertation

The dissertation consists of an introduction, five chapters, a conclusion and appendices, which present theoretical research, developed models and results of simulation experiments, as well as a comparative analysis of various control methods. The main text is 214 pages long, and the appendices, containing results of the conducted research and transient processes, are 64 pages long.

CHAPTER I

STATE OF THE PROBLEM. DEVELOPMENT OF ELECTRO-HYDRAULIC DRIVE SYSTEMS

1.1 Overview of modern electro-hydraulic tracking systems

A large part of modern industrial facilities include in their structures a number of hydraulic and pneumatic systems and mechanisms. Of the technical means ensuring the drive of industrial systems, the best characteristics are possessed by electro-hydraulic mechanisms, combining electrical input and hydraulic output units. The advantages of these drive mechanisms arise from the integral approach to implementation, based on the effective use of the capabilities of electrical and hydraulic systems. On the one hand, the structure of electro-hydraulic mechanisms uses the capabilities of electrical control systems with feedback, and on the other - the characteristics of hydraulic systems, associated with achieving maximum mechanical power. The studies conducted on electric, hydraulic and pneumatic drives show that only hydraulic drives are capable of developing significant mechanical power with small masses and dimensions. In today time is especially the development and improvement of electro-hydraulic actuators is important because because of their own advantages enter everything wider in the schemes on various robotic complexes, flexible automated production systems, road and construction machinery, machines and systems in ship and airplane industry, railway and the automobile transport and etc.

1.2 Electrohydraulic tracking systems

Despite their undeniable qualities, these systems have a number of disadvantages that limit their wider application. Their main disadvantages are the following:

- greater requirements for the accuracy of manufacturing the drive elements, since the leakage and loss of the working fluid, and therefore the values of the dynamic characteristics and Efficiency - it of the mechanisms;

- the significant nonlinearity of the elements of the electro-hydraulic drive systems;

- the dependence of the main characteristics of the drive on the temperature and degree of contamination of the working fluid;

- the dependence of the speed of the output unit on the mass of the load. There are two approaches to eliminating the above-listed disadvantages, which are expressed in the following ;

- improvement of the designs of individual elements, as well as the overall structure of the drive mechanism;

-development of electronic means for correction of the electro-hydraulic drive (improvement of the control system).

The complexity and significant losses in the implementation of a large part of the constructive solutions, in most cases, make the application of the second approach far more effective. In addition, drive systems based on this approach are characterized by simplified designs and high reliability, because their circuits lack moving mechanical elements.

With the advent of electrical feedback on the state variables of drives, the complexity of control systems increases significantly. Since it is necessary to take into account nonlinear effects and the change of basic parameters over time, modern electro-hydraulic drive systems are designed based on the latest advances in the field of technical systems control.

1.2.1 Structure of electro-hydraulic tracking system

Hydraulic and electro-hydraulic actuators are widely used in the automation of many processes in industry, transport and aviation. systems. With development on this direction are is isolated three basic type closed systems for regulation, respectively on position, speed and strength, as in the last In recent years, electrohydraulic systems with volumetric control of these parameters have been increasingly used [1] . In this case, it is avoided the main disadvantage of the systems with throttle regulation, a namely relatively the big ones losses on energy. The hydraulic system usually consists of several main components: a reservoir to carry the hydraulic oil, a pump to move the oil through the system at a specified flow rate, an electric motor or other power source to drive the pump with the appropriate torque, a distributor to regulate the direction, pressure and flow rate of the oil, an actuator for converting oil pressure into mechanical force or torque, to perform useful work (these are usually hydraulic cylinders or hydraulic motors) and a piping system that carries the oil from one place to another.

In the most common cases An electro-hydraulic or electro-pneumatic system includes the following main elements [1]:

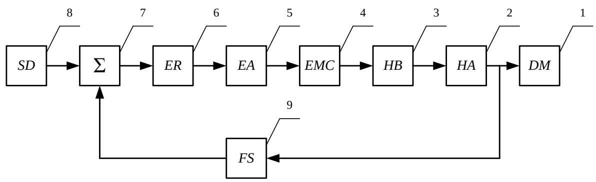

Fig. 1.1. Schematic diagram of an electrohydraulic tracking system

Fig. 1.1 presents a schematic diagram of an electro-hydraulic tracking system, the following elements are indicated on it : 1 - driven machine; 2 – hydraulic actuator; 3 - hydraulic booster; 4 - electro-mechanical converter; 5 - electric amplifier; 6 - electronic regulator; 7 - summing device; 8 - setting device; 9 - feedback sensor.

According to the control system, electro-hydraulic actuator systems are divided into open-loop and closed-loop systems. In open-loop systems, there is no feedback and the performance is based on the characteristics of the individual components of the system. The open-loop system is not accurate and the error can be reduced by proper calibration and control. The closed-loop system uses feedback, through a sensing element. The signal from the actual output is compared with the desired output and an error signal is given to the control element. The error is used to change the actual output and approach the desired value. Typically, closed systems use electro-hydraulic elements and digital electronics.

In order to more clearly highlight the features, advantages and limitations of the different approaches, a comparative analysis of the main control methods used in electro-hydraulic tracking systems has been carried out. The results of the analysis are presented in Table 1. 2 .

Table 1.2. Comparative analysis of different approaches to control electro-hydraulic tracking systems

Management method	**Advantages**	**Disadvantages**	**Robustness**	**Adaptability**	**Computational complexity**	**Apply - bridge for nonlinearities**
PID	Simple structure; easy implementation; low computational complexity	Sensitivity to parametric changes; limited effectiveness with nonlinearities	Low	Low	Low	Limited
Fuzzy	Good performance on nonlinearities; does not require an exact model	Complexity in selecting rules and membership functions	Medium	Medium	Medium	Good
Fuzzy - PID	Combines the advantages of *PID* and *Fuzzy* control; improved dynamic characteristics	More complex setup; rule base dependent	Good	High	Medium to high	High

Neural control	Ability to self-learn and adapt	High computational complexity; requires a lot of training	High	Very high	High	Very good
Neuro-fuzzy control	High adaptability ; good work under uncertainty	Complex structure; difficult to implement in real time	High	Very high	High	Very good
H $_\infty$ control	High robustness ; resistance to disturbances and uncertainties	Need for an accurate model; complex synthesis	Very high	Limited	High	Good

From the comparative analysis presented in Table 1. 2 it can be seen that classical *PID* controllers are characterized by a simple structure and easy practical implementation, but show limited efficiency in the presence of nonlinearities and parametric uncertainties . On the other hand, intelligent control methods based on fuzzy logic and neural networks provide better adaptability and stability under variable operating conditions, but are associated with increased computational complexity and more complex tuning.

The analysis shows that hybrid structures of the *Fuzzy – PID type* represent an effective compromise between control quality, adaptability and practical feasibility. Robust $H\infty$ controllers, in turn, provide high resilience to external disturbances and uncertainties, which makes them suitable for electro-hydraulic systems with dynamically changing parameters.

The obtained results justify the need to develop and research combined intelligent and robust approaches for controlling electro-hydraulic tracking systems.

1.4. Conclusions on the first chapter

The literature review shows a lack of a comprehensive approach combining modeling, identification and control of the EHTS, insufficient research of different operating modes, limited use of nonlinear models and incomplete consideration of the interactions between the elements of the system. A lack of sufficient quantitative justification for the adjustment of the regulators was also found.

It has been found that intelligent and hybrid control methods have significant potential for improving the dynamic characteristics of EHTS, but there is still a lack of a unified methodology for their design, tuning and robustness assessment, especially for systems with a rotary actuator.

CHAPTER II

MATHEMATICAL MODEL OF AN ELECTROHYDRAULIC TRACKING SYSTEM WITH A ROTARY ACTUATOR MECHANISM

2.1 Electrohydraulic tracking system diagram

Fig. 2.1 shows the diagram of an electro-hydraulic tracking system with a rotary actuator and a hydraulic loading subsystem.

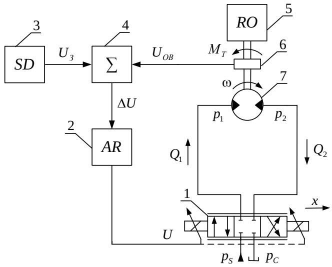

Fig. 2.1. Schematic of the electrohydraulic tracking system

The elements of the electrohydraulic monitoring system are as follows: 1 – proportional valve; 2 – automatic regulator; 3 – setting device; 4 – summing device; 5 – regulated object; 6 – speed sensor; 7 – hydraulic motor.

The task of the monitoring system is to move the object of regulation (a given machine) according to a certain law, overcoming all resistance forces and performing some useful work.

When the set voltage increases, U_3 the signal is processed by the summing device and the automatic regulator and is fed to the input of the proportional distributor. The plunger of the proportional distributor moves in the direction of increasing the throttling gap, in which the flow rate Q_1 to the motor increases and the angular velocity ω increases until a new set value is reached. When the U_3 process decreases, the process proceeds similarly in the opposite direction. When the load moment changes, M_T for example, by increasing it, the angular velocity of rotation of the hydraulic motor shaft initially ω decreases, which leads to a decrease in the feedback voltage U_{OB}, as a result of which an error is formed ΔU in the summing device, the signal is processed by the automatic regulator and the voltage U at the input of the proportional distributor increases. This leads to the movement of the plunger of the proportional distributor in the direction of opening the throttling gap and an increase in the flow rate Q_1 to the input of the hydraulic motor. When a control voltage with the opposite sign is applied to the proportional distributor, the direction of rotation of the hydraulic motor shaft changes and the process is analogous. As a result, the angular velocity ω increases, and the process continues until it reaches its initial value or close to it.

2.2 Equations describing the dynamics of the electrohydraulic system

2.2.1 Equation for the rotation of the hydraulic motor shaft

$$J\frac{d\omega}{dt} + k_{TP}\,\omega = w\,p_M - M_T \tag{2.2}$$

2.2.2 Flow equations flowing through the distribution device

The flow rates Q_1 and Q_2 flowing through the distributor are functions of the displacement x of the plunger and the corresponding pressure drop. For the equations of the flow rates passing through the distributor, according to Fig. 2.1, the following dependencies are valid:

for $x \geq 0$(plunger moves to the right):

$$Q_1 = \mu_1 S_1(x)\sqrt{\frac{2(p_S - p_1)}{\rho_1}} \tag{2.3}$$

$$Q_2 = \mu_2 S_2(x)\sqrt{\frac{2(p_2 - p_R)}{\rho_2}} \tag{2.4}$$

for $x < 0$(plunger moves to the left):

$$Q_1 = \mu_1 \, S_1(x) \sqrt{\frac{2(p_1 - p_R)}{\rho_1}} \tag{2.5}$$

$$Q_2 = \mu_2 \, S_2(x) \sqrt{\frac{2(p_S - p_2)}{\rho_2}} \tag{2.6}$$

With the same shape of the fluid flow cross-sections, it can be assumed that $\mu_1 \approx \mu_2 = \mu$, $\rho_1 \approx \rho_2 = \rho$, and $\Delta p_1 = p_S - p_1 = \Delta p_2 = p_2 - p_R = \Delta p$. After transforming (2.3) and (2.4) for the average flow rate Q , $Q = 0.5\,(Q_1 + Q_2)$, we obtain:

$$Q = \mu \pi d \, x \sqrt{\frac{p_S - p_M - p_R}{\rho}} \tag{2.7}$$

where $p_M = p_1 - p_2$is the pressure drop in the hydraulic motor.

2.2.3 Equations for the flow rates entering the left (right) side of the hydraulic motor

For the flow rates that enter the hydraulic motor and determine the pressure change, the fluid continuity equations are written, taking into account the compressibility of the liquid:

$$Q_1 = w\,\omega + \frac{V_{01}}{B}\frac{dp_1}{dt}\,sign(x) \tag{2.8}$$

$$Q_2 = w\,\omega - \frac{V_{02}}{B}\frac{dp_2}{dt}\,sign(x) \tag{2.9}$$

Assuming symmetry, that $V_{01} \approx V_{02} = V_0$, $d_1 = d_2 = d$ and $L_1 = L_2 = L$, and identical initial conditions, for the average flow rate Q we obtain:

$$Q = w\,\omega + \frac{V_0}{B}\frac{dp_M}{dt}\,sign(x) \tag{2.10}$$

2.2.4 Summing device equation

The summing device forms an error signal ΔU the difference between the reference voltage U_3 and the feedback voltage U_{OB}:

$$\Delta U = U_3 - k_{OB}\omega \tag{2.12}$$

2.2.5 Electronic *PID* controller equation

The analog or digital *PID* controller implements proportional, integral and derivative action on the error ΔU

$$U = k\left(\Delta U + \frac{1}{T_i}\int \Delta U \, dt + T_d \frac{d\Delta U}{dt}\right) \tag{2.13}$$

Here, the proportional term responds to the current error, the integral term eliminates the static error, and the differential term improves response and stabilizes the system by predicting the change in the error.

2.2.6 Equation for displacement of the proportional valve plunger

The proportional distributor is described by first-order dynamics (neglecting higher frequencies):

$$T_u \frac{dx}{dt} + x = k_u U \tag{2.14}$$

2.3 Structural diagrams. Transfer functions.

The set of equations (2.2), (2.3), (2.4), (2.5), (2.6), (2.7), (2.12) (2.13) and (2.14) describes the operation of the closed-loop tracking system with throttle control in dynamic mode.

2.3.3 Laplace transform

After linearization around the operating point of equations – (2.2), (2.9), (2.10), (2.12), (2.13), (2.14), and application of the Laplace transform under zero initial conditions for the deviations, the equations obtain the operator form (notations Δ omitted for brevity):

$$\left(J s + k_{TP}\right) \omega(s) = w p_M(s) - M_T(s) \tag{2.25}$$

$$Q(s) = k_x x(s) - k_p p_M(s) \tag{2.26}$$

$$Q(s) = w \omega(s) + \frac{V_0}{2B}(s) p_M(s) \tag{2.27}$$

$$\Delta U(s) = U_3(s) - k_{OB}\, \omega(s) \tag{2.28}$$

$$U(s) = k\left(1 + \frac{1}{T_i s} + T_d s\right) \Delta U(s) \tag{2.29}$$

$$\left(T_u s + 1\right) x(s) = k_u U(s) \tag{2.30}$$

2.3.4 Structure diagrams

Based on the transformed model in operator form (2.25), (2.26), (2.27), (2.28), (2.29) and (2.30), the structural diagram of the system was developed, which is presented in Fig. 2.3.

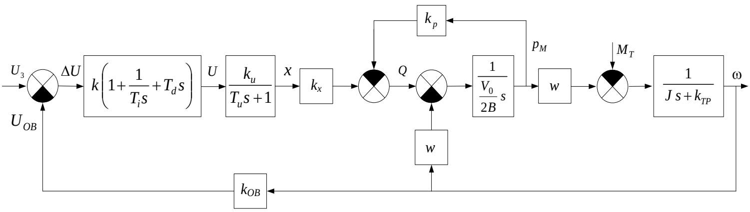

Fig. 2.3 System block diagram

The scheme contains several closed loops (an inner pressure loop and an outer velocity loop). To avoid overlapping feedback loops, by equating equations (2.26) and (2.27) and eliminating $p_M(s)$and, $Q(s)$the transformed scheme in Fig. 2.4 is obtained.

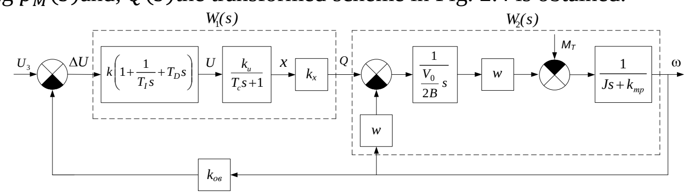

Fig.2.4 Converted system structure diagram

After successive transformations (Fig. 2.4), the transfer functions are reached.

Transfer function of the open system (the ratio of the output quantity $\omega(s)$to the error $\Delta U(s)$in a broken feedback loop): $W(s)=\dfrac{\omega(s)}{\Delta U(s)}$

After transforming the structural diagram for the transfer function of the closed system, we obtain:

$$\Phi(s)=\frac{\omega\,(s)}{U_3(s)}=\frac{b_2 s^2+b_1 s+b_0}{a_4 s^4+a_3 s^3+a_2 s^2+a_1 s+a_0} \qquad (2.35)$$

2.3.5 System resilience area

The stability of the closed system is determined by the roots of the characteristic polynomial:

$$a(s)=a_4s^4+a_3s^3+\left(A_1+k_{OB}k_I A_2\right)s^2+\left(A_3+k_{OB}k_I A_4\right)s+a_0 \qquad (2.39)$$

For a fifth-order system, the stability conditions can be obtained using the Rauss-Hurwitz criterion. At the stability limit, the characteristic polynomial has purely imaginary roots $s = j\omega$. After substitution and separation of the real and imaginary parts, two equations are obtained:

$$a\,(i\omega)=X\,(\omega)+iY(\omega) \qquad (2.40)$$

where:

$$X(\omega)=a_0-a_2\omega^2+a_4\omega^4 \qquad (2.41)$$

$$Y(\omega)=a_1\omega-a_3\omega^3 \qquad (2.42)$$

For the system to be at the limit of stability, the following condition must be met:

$$X(\omega)=a_0-a_2\omega^2+a_4\omega^4=0 \qquad (2.43)$$

$$Y(\omega)=a_1\omega-a_3\omega^3=0 \qquad (2.44)$$

Taking into account (2.39) we obtain:

$$X\,(\omega)=k_{OB}k_i\,-\left(A_1+k_{OB}k_I A_2\right)\omega^2+a_4\omega^4=0 \qquad (2.45)$$

$$Y(\omega)=\left(A_3+k_{OB}k_I A_4\right)\omega-a_3\omega \qquad (2.46)$$

If from equation (2.46) is expressed $\omega^2=\dfrac{A_3+k_{OB}k_I A_4}{a_3}$ and substituted into equation (2.45), after introducing the notation $K=k_{OB}k_1$, we arrive at the equation:

$$B_1K^2+B_2K+B_3=0 \qquad (2.47)$$

where : $B_1 = a_4A_4 - a_3A_2A$; $B_2=2a_4A_3A_4+a_3\left(a_3-A_1A_4-A_2A_3\right)$; $B_3=a_4A_3^2$.

For the solution of the quadratic equation (2.47) we obtain:

$$K_{1.2} = \frac{-B_2 \pm \sqrt{D}}{4B_1} \tag{2.48}$$

where: $D = B_2^2 - 2B_1B_2$

Matlab program was developed to construct the stability region of the system , using the dependencies from (2.38) to (2.49). The resulting stability region is presented in Fig. 2.6.

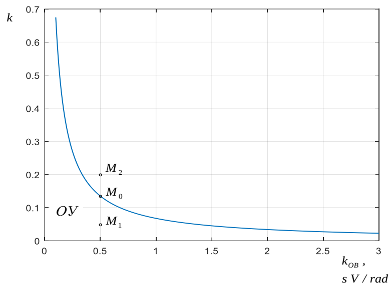

Fig. 2.6 . System stability region in terms of k and k_{OB}

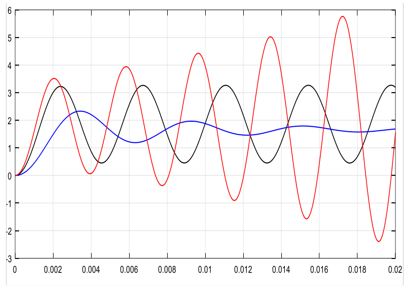

Fig 2.7 Transient processes in the system for different ordered pairs for k and k_{OB}

For each ordered pair k and k_{OB} From the curve shown in Fig. 2.6, the automatic system is at the stability limit. The stable region is indicated by OY, and the unstable region is located above the curve.

Fig. 2.7 presents transients for three ordered pairs for k and k_{OB} from Fig. 2.6 - t. M_0(0.5, 0.1352) , t. M_1(0.5, 0.0500) and t. M_2(0.5, 0.2000) , corresponding to a system at the stability limit - 1, stable - 2 and unstable system - 3. These results confirm the correctness of the linearized model and provide an opportunity to select the parameters of the regulator, ensuring stable operation with the desired quality.

2.4.1 Simulink model structure

Fig. 2.13 presents an analog model of an electrohydraulic tracking system with a rotary actuator in general form, without specifying the type of the loading subsystem.

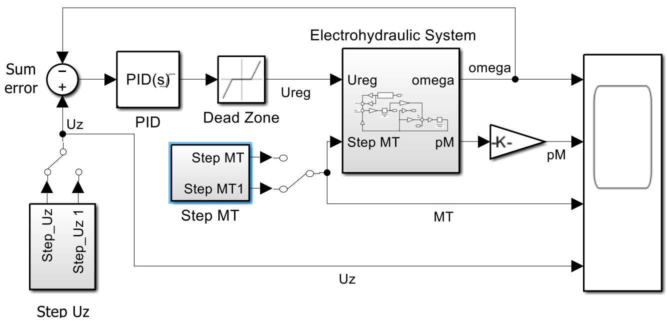

Fig.2.13 Analog model of an electrohydraulic tracking system with a rotary actuator.

The model consists of the following basic blocks (implemented in *Simulink*):

- **Stepper motor U_z** – generates a step, sinusoidal or arbitrary input signal $U_z(t)$(voltage in the range 0–5*V*).

- **Load block (Step M_T)** – generates a step or arbitrary step signal $M_T(t)$ 0–5V that models the external load (disturbance) on the system.

- **Sum error** – calculates the error:$\Delta U = U_z - k_{OB}\omega$

- ***PID* controller (*PID*)** – implemented as a continuous *PID* block with the ability to adjust the parameters k_p, $T_i$and T_d. An anti-windup mechanism is included by limiting the control signal.

- **Dead Zone** – nonlinearity with a symmetrical zone:$[-\Delta, \Delta]$, $\Delta = 2V$

Usually the dead band is applied to the displacement of the distributor. In the present model, for simplicity, it is applied to the control signal U_{reg}, since the coefficient $k_{\text{разп}}$is assumed to be linear.

2.4.3 Model verification

To validate the Simulink model, simulations were conducted at different values of the *PID* controller parameters and the feedback coefficient k_{OB}. Two main modes were investigated:

- **Transient processes on demand** – with a step change in the command voltage U_3 (for example, from 0 to 5*V*) and a constant load $M_T = const$;

- **Load transients** – with a step change in the load moment M_T(disturbance) and a constant setpoint$U_3 = const$

For compatibility of the simulation results and the real system, the angular velocity of the hydraulic motor shaft ω and the load moment M_T in the simulation model are given as stresses. The relationship is$1V \cong 150\,rpm$

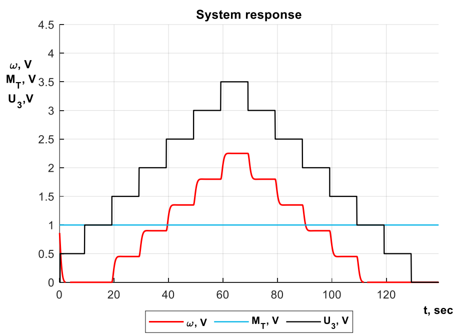

Fig. 2.15 Transient processes of the open system at $M_T = 1V$

Fig. 2.15 shows the transient processes of the open system when the setpoint changes in the interval $U_3 \in [0 \div 3.5]V$, respectively at $M_T = 1V$. The graphs show the presence of a dead zone (zone of insensitivity) at the beginning of the operating range, which is due to the positive overlap of the proportional distributor. Also, the setpoint is not reached - the presence of a static error in the established mode, caused by the lack of integral action in the regulator (in an open system) or by insufficient amplification in a closed loop without an integrator.

2.4.4. System research by assignment

Below are the results of simulations in *MATLAB/Simulink* for four variants of *PID* controllers , whose parameters are summarized in Table 2.2 . The studies were conducted with a step change in the reference voltage. U_3:with size $0.5V$in the interval $[0,3.5]V$and constant disturbance $M_T = 0V$.

Table 2.2. Parameters of the studied regulators

Variant	K_p	$K_i[s]$	$K_d[s]$	Characteristics
Option A (Fig. 2.18)	0.5819	1.214	0.01	Slow, aperiodic
Option B (Fig. 2.19)	1.2494	2.3222	0.1331	Optimal compromise
Option C (Fig. 2.20)	2.676	4.097	0.4326	With overregulation
Option D (Fig. 2.21)	88.0	3.3	0.01	Near the limit of sustainability

Objective of the study: To compare the behavior of the system at different *PID* controller settings in terms of response speed, overshoot, static error and stability.

Character: Aperiodic, slow.

Rise time (10%–90%): ≈ 1.9 s.

Settling time (±2%): ≈ 2.98 s.

Override: 0%.

Error detected: 0 (thanks to the integrator).

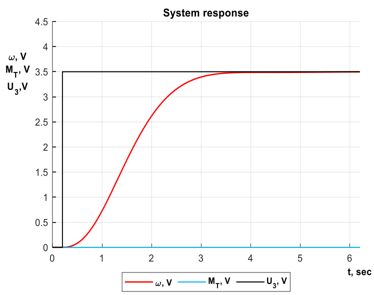

Fig. 2.18 Option A:($K_p = 0.5819, K_i = 1.214s^{-1}, K_d = 0.01\ s$)

1. Influence of odds

- **K_p = 0.5819** – low proportional gain, which leads to weak error response. The distributor plunger moves slowly.

- **K_i = 1.214s^{-1}** – relatively low integral coefficient; the accumulation of the integral signal is slow, which extends the time for eliminating the static error (although it eventually reduces it to 0).

- **K_d = 0.01s** – very small differential coefficient, almost no effect on dynamics.

2. Sustainability and stocks

The setting is deep in the stable region, with a large phase margin (> 80°). The system is absolutely stable even with significant changes in parameters (deterioration of oil viscosity).

3. Advantages

- Zero overshoot – ideal for applications sensitive to mechanical shocks (e.g. driving expensive optical systems, elevators with loads).

- Robustness – parameters can be doubled without the system losing stability.

4. Disadvantages

- Very slow job processing ($t_s \approx 3s$) – unacceptable for processes with frequent changes (e.g. robot tracking systems).

- Low gain leads to high sensitivity to friction in the hydraulic motor - in the presence of static friction (stiction), the error can persist for a long time before the integrator overcomes it.

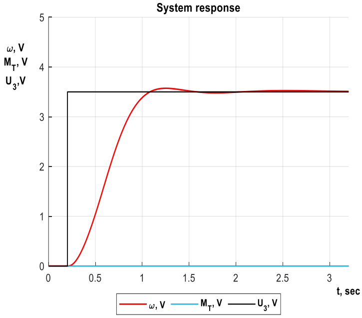

Fig. 2.19 Option B:$\left(K_p = 1.2494, K_i = 2.3222\ s^{-1}, K_d = 0.1331\ s\right)$

Character: Fast, weak overshoot.

Rise time (10%–90%): ≈ 0.9 s.

Settling time (±2%): ≈ 1.4 s.

Overshoot: ≈ 2.08%.

Error detected: 0

1. Influence of coefficients on dynamics

- Proportional coefficient (K_p=1.2494) – increased approximately 2.15 times compared to option A. This leads to a higher error amplification, which shortens the rise time from 1.9 s to 0.9 s (more than twice as fast).

- Integral coefficient ($K_i = 2,3222s^{-1}$) – increased by 1.91 times. It provides rapid elimination of the static error, but does not cause additional overregulation, because the integrator is balanced by the differential component.

- Differential coefficient ($K_d = 0,1331s$) – increased 13 times compared to option A. This is the key to the improvement: the differential component "extinguishes" the inertia of the system, reducing the overregulation from potentially over 8–10% (in the absence of K_d) to only 2.08%.

2. Sustainability and stocks

Placed on the stability diagram (Fig. 2.6), the parameters of option B lie deep in the stable region , with good margins in amplitude and phase:

- Phase margin ≈ 45° – 55°

- Amplitude margin ≈ 6 – 10 dB

This ensures robustness to changes in load and oil temperature.

3. Physical interpretation in the hydraulic system

- Higher $K_p$means that the proportional valve receives a larger control signal for the same error - the plunger moves faster and the flow rate to the motor increases sharply.

- The differential component ($K_d = 0{,}1331$) provides a preliminary "braking" before reaching the setpoint, which prevents inertial overspeeding. This is especially important for hydraulic motors with low fluid compressibility.

- The integral signal accumulates quickly, but due to the limitations of the output signal (saturation is not reached), there is no danger of windup.

4. Assessment of robustness to load changes

Additional simulations were conducted with $M_T$from 0 to 3V :

- At nominal load (1.5V) , the settling time increases to 1.7s, and the overshoot to 2.5%.

- At maximum load (3V) the system remains stable and achieves the setpoint in ~2.1s with overshoot below 3%.

- These results confirm **the robustness** of variant B under significant load variations.

5. Disadvantages and limitations

- There is still a slight overshoot (2.08%), which is not acceptable in some specialized medical or aerospace applications.

- The differential component ($K_d = 0{,}1331$) amplifies high-frequency noise from the speed sensor. In installations with noisy feedback, an additional low-pass filter may be required.

- The parameters were obtained by simulation under nominal conditions; in case of significant change in oil viscosity (e.g. during cold start) a slight correction of may be necessary K_d.

Conclusion: Option B represents a golden mean for a wide range of industrial electrohydraulic tracking systems. It combines high response speed ($t_s < 1{,}5s$), small overshoot (< 3%), zero static error and good robustness to load changes. It is recommended as the first choice when designing positioning, speed tracking and active vibration protection systems.

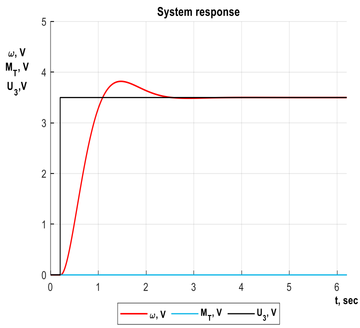

Fig. 2.20 Option C:$\left(K_p = 2.676, K_i = 4.097s^{-1}, K_d = 0.4326s\right)$

Character: Fast, with significant overshoot.

Rise time (10%–90%): ≈ 0.64 s.

Settling time (±2%): ≈ 2.04 s.

Overshoot: ≈ 9.12%.

Error detected: 0

1. Influence of odds

-$\boldsymbol{K_p = 2,676}$– more than twice as high as option B. This sharply increases the steepness of the front face ($t_r = 0{,}64s$).

-$\boldsymbol{K_i = 4,097s^{-1}}$– a high integral coefficient that quickly eliminates static error, but contributes to overregulation because the integrator continues to accumulate signal while the system passes the setpoint.

- $\boldsymbol{K_d = 0,4326s}$– significant differential action that attempts to slow the system down before the setpoint. However, due to the high $K_p$and K_i, the effect is not sufficient to completely suppress overshoot.

2. Sustainability and stocks

The system is close to the stability limit (Fig. 2.6). The phase margin is about 25–30°, the amplitude margin – about 4–6 *dB*. Small changes in the parameters (for example, decreasing $T_{\text{разп}}$or increasing V) can lead to instability.

3. Dynamic characteristics

- After the initial rapid jump (0.64s), the system passes the setpoint by about 9%. The settling time (2.04s) is longer than option B due to the presence of decaying oscillations (2–3 periods with small amplitude). The return to the setpoint occurs with a time constant of ≈ 0.5s after the first maximum.

4. Advantages

- Fastest rise time among the considered options – suitable for systems requiring high acceleration (e.g. impact testing). Good interference suppression due to high gain.

5. Disadvantages

- Significant overshoot (9%) – unacceptable for precise positioning (metal cutting machines).

- Risk of overloading the hydraulic motor at peak torque, which is proportional to $K_p \cdot e_{max}$.

- Requires careful sizing of the proportional valve (rate of flow increase).

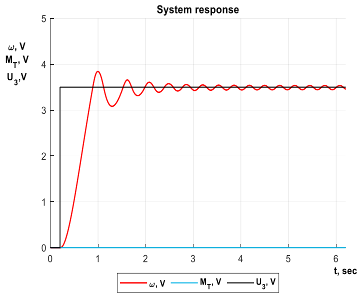

Fig. 2.21 Option D:$\left(\mathrm{K_p} = 88.0, \mathrm{K_i} = 3.3\ s^{-1}, \mathrm{K_d} = 0.01s\right)$

Character: Weakly damped oscillations – the system at the limit of stability.

Rise time (10%–90%): < 0.3s.

Settling time (±2%): not reached – constant fluctuations with amplitude ≈ ±1.26% around the setpoint.

Overshoot: ≈ 9.8% (first maximum).

Error detected: average value 0, but with undamped fluctuations.

1. Influence of odds

- $\boldsymbol{K_p = 88}$ – extremely high proportional gain (70 times over option B). This results in an almost instantaneous response, but causes overshoot and subsequent oscillations.

- $\boldsymbol{K_i = 3,3s^{-1}}$ – a moderate integral coefficient, which in combination with the large one K_p creates an almost pure integral-proportional behavior with little damping.

- $\boldsymbol{K_d = 0,01s}$ – negligible differential action → no stabilizing ingredient.

2. Sustainability and stocks

According to Fig. 2.6, the pair ($K_i, K_{\text{обр}}$) for option D lies on or above the stability curve

.

- Phase margin ≈ 0° – 5° (practically zero).

- Amplitude margin ≈ 1 – 2 dB.

- The system is in **a limit cycle mode** – small changes (e.g. noise in the feedback) make it unstable.

3. Advantages

- Extremely fast initial response – $t_r < 0{,}3s$.

- Can be used for theoretical analysis of boundary resistance.

4. Disadvantages

Unacceptable for practical use – unrelenting oscillations lead to wear of hydraulic components, noise, vibrations and inability to achieve accurate positioning.

- Small changes in load or oil temperature will cause a transition to instability (increasing fluctuations).

- The proportional valve operates in a constant switching mode, which shortens its life.

5. Recommendations

- Do not use option D in real systems.

- It serves only as **an example of the stability limit** – if such undamped oscillations appear during adjustment, K_P should be immediately reduced by at least 5–10 times.

- To achieve such fast response without oscillations, it is recommended to use a cascade controller or an adaptive algorithm (*Fuzzy-PID*).

Conclusion: For the studied electrohydraulic tracking system with a rotary actuator, Option B: $\left(\mathrm{K_p} = 1.2494, \mathrm{K_i} = 2.3222\ s^{-1}, \mathrm{K_d} = 0.1331s\right)$provides the best balance between fast response ($t_s \approx 1{,}4s$), small overshoot ($\approx 2\%$), and zero static error. It is recommended for practical implementation.

2.4.5. System testing under load change

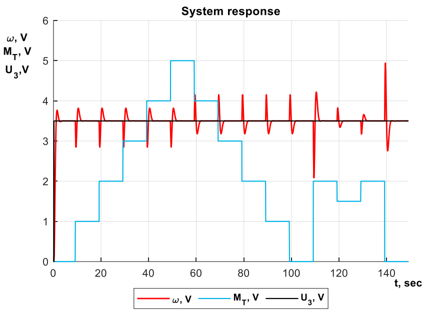

Fig. 2.22. Transient processes when changing the load in the range 0 – 4 V and a constant setpoint$U_3 = 3.5V$

The study of the behavior of a system under load changes is a key stage in the analysis of its stability, efficiency and reliability. It allows to trace how system parameters – such as voltage, current, frequency, pressure or flow rate – react to an increase or decrease in the required power or performance. This analysis reveals the operating limits of the system, potential risk zones of overload and its ability to recover from disturbances.

Analysis of option B with $U_3 = 3{,}5V$and change in load moment M_T
Experimental conditions

- **Set voltage:** $U_3 = 3{,}5V$(constantly)
- **Desired angular velocity:** $\omega_{\text{жел}} = U_3 \cdot k_{\text{обр}} = 3{,}5 \times 0{,}3 = 1{,}05 rad/s$
- **PID controller parameters (option B):**

$$K_p = 1{,}2494, K_i = 2{,}3222s - 1, K_d = 0{,}1331s$$

- **Perturbations studied:** step changes of M_T: $0 \to 1\ V,\ 0 \to 2\ V,\ 0 \to 3V$ and reverse step$3 \to 0V$

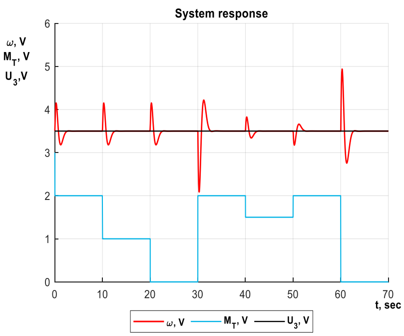

Fig.2.23 . The system response to a load change of 1,2 and 3V

Fig. 2.23 shows the response of the system to a load change of 1, 2 and 3V.

1. Load step$0 \to 1V$

- **Angular velocity drop:** ≈ 3.2% (from 1.05 rad/s to 1.016 rad/s)

- **Recovery time (up to ±2% of the setpoint):** ≈ 1.5s

- **Override on return:** none

- **Static error after recovery:** 0

Analysis: The small disturbance is compensated quickly due to the high integral gain (K_i). The differential component (K_d) prevents overregulation. The system behaves as quasi-static – the deviation is negligible.

2. Load step $\mathbf{0} \rightarrow \mathbf{2}\boldsymbol{V}$

- **Angular velocity drop:** ≈ 7.8% (up to 0.968 rad/s)

- **Recovery time:** ≈ 1.9s

- **Overshoot:** ≈ 1.2% above setpoint on return

- **Static error:** 0

Analysis: Increasing the load leads to a more noticeable drop, but the system remains stable. Recovery takes less than 1s. A small overshoot (1.2%) is acceptable. Compared to option A (with the same load, the drop would be >15% and recovery time >2 s), option B shows significantly better robustness.

3. Load step $\mathbf{0} \rightarrow \mathbf{3}\boldsymbol{V}$(maximum tested load)

- **Angular velocity drop:** ≈ 14.5% (up to 0.898 rad/s)

- **Recovery time:** ≈ 3.3s

- **Overshoot:** ≈ 3.5% above setpoint

- **Static error:** 0

Analysis: At maximum load the deviation reaches 14.5%, which is still within the acceptable limits for most industrial applications. The recovery time (3.3s) is about twice as long as in the absence of load (1.4s per task), but the system does not lose stability. The overshoot of 3.5% is insignificant. A comparison with option C (which at the same load would have a drop of ≈ 10% but overshoot >8% and slight fluctuations) shows that option B offers a smoother and more predictable behavior.

4. Reverse load step3 $\rightarrow \mathbf{0}\boldsymbol{V}$

- **Angular velocity increase:** ≈ +12% (up to 1.176 rad/s)

- **Recovery time:** ≈ 2.0s

- **Overshoot:** none (monotonic return)

- **Static error:** 0

Analysis: When the load is suddenly removed, the system does not exceed the setpoint – the differential component successfully delays the reaction, preventing overregulation. This is important for mechanisms sensitive to accelerations (for example, when working with fragile materials).

Influence of PID parameters on load:

- $\boldsymbol{K_p = 1,2494}$– provides a sufficiently fast response to the error, but does not cause excessive amplification, which would lead to sensitivity to noise.

- $\boldsymbol{K_i = 2,3222 s^{-1}}$– the high integral constant allows for rapid elimination of the static error, but does not cause integral windup because the *PID* output is limited (an upper limit of $10V$ is set in the model).

- $\boldsymbol{K_d = 0,1331}s$– the differential component plays a key role in suppressing overshoot after a disturbance. Without it (at $K_d = 0$) the drop at $3V$ would be the same, but the return would cause an overshoot of about 8–10%.

Robustness assessment:

The change in oil temperature (from 20°C to 60°C) leads to a decrease in viscosity and a corresponding decrease in k_{TP} by about 30%. Simulations show that in option B the recovery time increases by 0.3s, and the overshoot – by 3.5%. The system remains stable. In option C the same change leads to a loss of stability (damping oscillations with an amplitude of 5% appear). This confirms the higher robustness of option B.

Conclusion for option B when changing the load

Option B demonstrates excellent load disturbance compensation capability . Option B is recommended for systems operating under frequently changing loads (hydraulic robot drives, test benches, active suspensions).

CHAPTER III

EXPERIMENTAL STUDIES OF THE AUTOMATIC ELECTROHYDRAULIC TRACKING SYSTEM WITH CLASSIC REGULATORS

3. 1 Description of the laboratory automated electrohydraulic system

The experimental studies of the electrohydraulic tracking system with a rotary actuator were conducted on the developed laboratory stand "Automated system for the study of hydraulic and thermal processes", which is located on the territory of the Department of Power Engineering at Gabrovo Technical University.

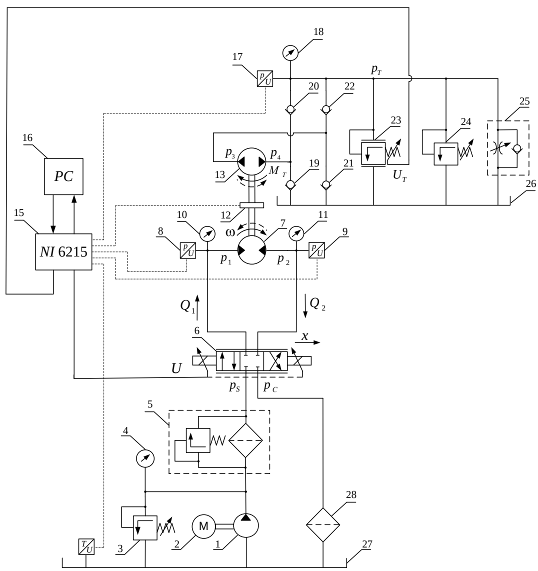

Fig. 3.1 Schematic of the electrohydraulic tracking system

When the system starts , voltage is supplied to electric motor 2. Pump 1 sucks working fluid from tank 27. and feeds it to the pressure main. The fluid passes through a high-pressure filter with a safety valve 5 installed and reaches the inlet of the proportional distributor 6. The required pressure in the system is guaranteed by the settings of the safety valve 3, through the readings of the pressure gauge 4. The hydraulic system is ready and waits for the supply of control voltage to the proportional distributor. In an established operating mode, a certain value of the control voltage U_3 corresponds to a certain angular speed ω of rotation of the hydraulic motor shaft. When increasing the setting voltage U_3 , the signal is processed by the summing device and the automatic regulator and enters the input of the proportional distributor. The plunger of the proportional distributor moves in the direction of increasing the throttling gap, whereby the incoming flow rate Q_1 to the hydromotor increases and the angular velocity ω increases until a new set value is reached. When decreasing, U_3 the process proceeds similarly in the opposite direction. When the load moment changes M_T , for example, increasing, initially the angular velocity of rotation of the hydromotor shaft ω decreases, which leads to a decrease in the feedback voltage U_{OB} , as a result of which an error is formed ΔU In the summing device, the signal is processed by the automatic regulator and the voltage U at the input of the proportional distributor increases. This leads to the displacement of the proportional distributor plunger in the direction of opening the throttling gap and increasing the incoming flow rate Q_1 to the inlet of the hydraulic motor.

When a control voltage with the opposite sign is applied to the proportional distributor, the direction of rotation of the hydraulic motor shaft changes and the process is analogous. As a result, the angular velocity ω increases, and the process continues until it reaches its initial value or close to it. The load moment in both directions of shaft rotation can be changed by the proportional support valve 23 remotely or by changing the setting of the adjustable throttle of the DROC 25 and the setting of the support valve 24. When the proportional support valve 23 is used, the adjustable throttle of the throttle with check valve 25 is fully closed, and the support valve 24 is set to operate at a higher pressure. When the support valve 24 and the throttle with check valve 25 are used, the proportional support valve 23 is fully closed. In one direction of pump rotation, the path of the hydraulic oil in the load direction is from the reservoir 26, through the check valve 21, through the left chamber of the gear pump 13, through the check valve 20 to the proportional support valve 23, the support valve 24, the throttle with check valve 25 and to the reservoir 26.

Fig. 3.2 presents a general view of the laboratory stand for real-time EHTS research. The control is carried out by a personal computer and a module for controlling the input and output signals - Fig. 3.4.

Fig. 3.2 Laboratory stand for EHTS research

Fig. 3.3 Power part of the laboratory bench

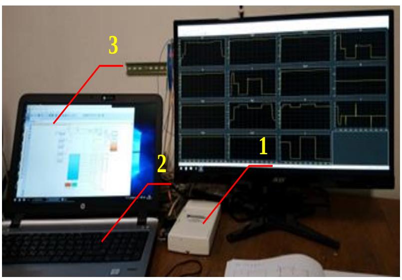

Fig. 3.4 Hardware and software control system of EHTS

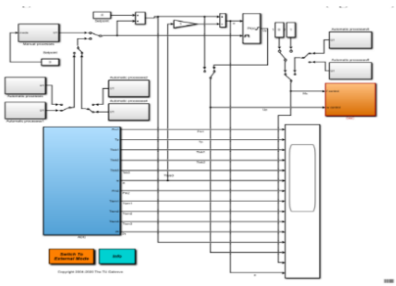

Fig. 3.5 Matlab Simulink model of a real-time process research system in the EHTS

The experimental complex consists of the following components of the electrohydraulic tracking system:

- loading module (Fig. 3.3 - object 1), including a hydraulic motor and a loading hydraulic subsystem;

- hydraulic station and control elements of the electro-hydraulic system (Fig. 3.2 - object 2);

- a control and data collection system consisting of a measuring module (Fig. 3.4 - object 1), a personal computer (Fig. 3.4 - object 2) and specialized software (Fig. 3.4 - object 3).

Fig. 3.4 and Fig. 3.5 present transient processes in real time and the developed model in *Matlab Simulink* .

3.1.1 Measurement hardware

The experimental stand is controlled by a personal computer with an installed *MATLAB environment* and *the Data Acquisition Toolbox™ package* **(**Fig. 3.4 object 2) which provide tools for collecting, processing and analyzing measurement data in real time, as well as for implementing and testing control algorithms.

The connection between the computer and the stand is made through a universal measurement module NI USB-6215 (Series Data Acquisition), (Fig. 3.4 object 1).

Through the analog inputs of the module, multi-channel measurement of the following quantities is implemented:

- Pressure sensors – 3 pieces, with current transmitters 4 – 20mA and measuring range 0 – 16MPa and accuracy ± 0.5 %;

- Temperature sensors – 7 pieces, type Pt100 with current transmitters 4 – 20mA, measurement range 0 – 100°C and accuracy ± 0.2°C;

- Angular velocity sensor – tachogenerator with output voltage in the range 0 –10*V*, proportional to the speed of rotation of the hydraulic motor shaft and is used to form the angular feedback speed . The hydraulic motor in the system operates at a nominal speed of 800 min $^{-1}$, and the voltage returned by the tachogenerator is about 5*V*.

The measured signals are entered into the *MATLAB/Simulink* environment via the Analog Input block provided by the Data Acquisition Toolbox™, which allows interactive configuration and execution of data acquisition sessions.

3.1.2 Control signals

The control signal is generated in the *Simulink environment* using an *Analog Output block* .

The control of the proportional distributor is implemented via analog output AO $_0$ of the *NI USB-6215* measuring module , to which supplies control voltage in the range from **-** 5*V* to + 5*V*. The system loading is implemented through a second analog output AO $_1$, which supplies a voltage in the range of 0 – 5*V* to the proportional safety valve. This allows for experiments in different operating modes.

The electro-hydraulic system has two control channels. The two channels are used to control the angular velocity of the hydraulic motor shaft and the loading pressure.

The error is formed by a signal from the tachogenerator, analyzed by the control system, and then fed to the input of the proportional distributor.

3. 2 Transitions in the automated monitoring system

3.2. 1 Transient processes in the open system

3.2.1.1 Transient processes in the open system by assignment

Fig. 3.6 shows a series of experimental transients in the following electrohydraulic system when the control voltage changes U_3 . Three zones of behavior are observed:

- **Dead zone:** When a voltage of $0V$ to $2V$ *is applied* , the hydraulic motor shaft does not rotate. This is due to **the positive overlap** of the proportional valve plunger – a typical design non-linearity that leads to a delay in response.

- **Linear operating region:** In the range $2V - 4.5V$, the shaft angular velocity increases almost proportionally to the input voltage. This allows the application of linearized models for regulator synthesis.

- **Saturation zone:** When $U_3 > 4.5V$ the output signal (angular velocity) reaches a maximum – the throttle gap of the distributor is fully open. The system goes into a limiting mode, which leads to zero differential gain and the inability to further increase the angular velocity.

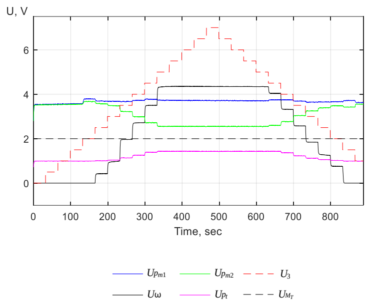

Fig.3.6 Transient processes of an open system under changing U_3 and constant load $U_{M_T} = 2V$

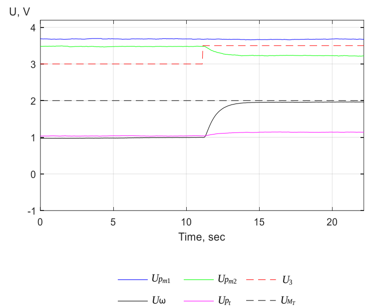

Fig.3.8 Transient processes of an open system when changing U_3 and at constant load $U_{M_T} = 2V$

Fig. 3.8 shows a transient process of the automated tracking system when the U_3 from $3V$ to $3.5V$ (period from $200s$ to $220s$), at a constant load voltage $U_{M_T} = 2V$. In this range:

- **The operating point is in the middle of the linear range** . The transient process occurs with greater steepness, since the gain of the proportional distributor is maximum.

- **Rise time (10%→90%):** approximately $2s$ – faster than the previous jump.

-**No overregulation caused by the inertia of the hydraulic motor and the compressibility of the working fluid is observed** when the valve is suddenly opened.

- The transient process is stable and aperiodic – without visible fluctuations, which indicates good damping of the system.

3.2.1.2 Open system load transients

Fig. 3.12 shows a series of experimental transients in the following electrohydraulic system when the load voltage changes U_{M_T} in the range of $0V$ up to $6V$ with a step of $0.5V$ and $1V$ constant setting voltage $U_3 = 3V$.

This series of dynamic processes is characterized by:

- **Influence of load on speed:** When the load voltage increases from $0V$ to $4.5V$, the angular velocity of the hydraulic motor shaft **decreases** monotonically. This is due to the proportional safety valve, which, when the control voltage increases, increases the discharge of working fluid (or increases the pressure against the motor), which loads the hydraulic motor.

- **Linear load regulation zone:** In the range $0 - 4.5V$ the dependence $U_{M_T} \to U_{\omega}$. is approximately linear, with a negative gain (increasing load → decreasing speed).

- **Load saturation zone:** At $U_{M_T} > 4.5V$ the shaft speed remains constant (minimum but non-zero) because the throttling gap of the proportional safety valve is maximally open and further increase in voltage does not change the hydraulic resistance.

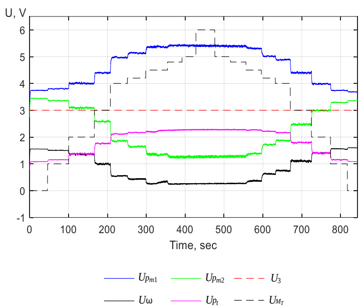

Fig.3.12 Transient processes of an open system when changing the load U_{M_T} at constant input voltage $U_3 = 3V$

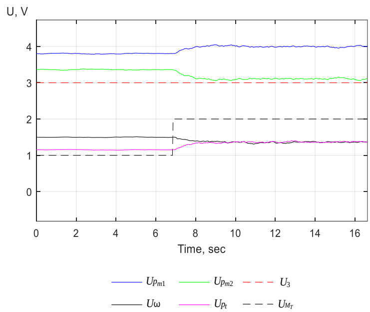

Fig.3.13 Transient processes of an open system when changing the load U_{M_T} at constant input voltage $U_3 = 3V$ for the period of 85*s* up to 100 *seconds*

- **Hysteresis when reducing the load:** When reducing U_{M_T} from $4.5V$ to $0V$, the speed increases, but due to hysteresis in the safety valve, the return curve does not coincide with the increase curve. This leads to a difference in speed at the same load voltage depending on the direction of change.

Fig. 3.13 shows a transient process of the automated tracking system when the U_{M_T} from $1V$ to $2V$ (period from 85s to 100s), at a constant set voltage $U_3 = 3V$. When voltage is applied to the proportional safety valve, the hydraulic motor shaft reduces the angular velocity corresponding to the readings of the speed sensor. This is a small increase in the load at the lower end of the range. The speed decreases by about 5–8% of the nominal. The transient process is aperiodic with a fall time (90%→10%) of approximately 1.2s. There is no overshoot – the system smoothly reaches the new lower speed.

Conclusions :

1.Load control via a proportional safety valve allows smooth adjustment of the speed of the hydraulic motor over a wide range, but provided that the control voltage is above the insensitivity zone ($U_3 > 2V$).

2.The presence of a dead zone and hysteresis in the safety valve leads to an uneven response to load increases and decreases, which must be compensated for by the closed loop.

3. Important note: The load experiments (Fig. 3.12 – Fig. 3.19) were carried out at a fixed setpoint voltage $U_3 = 3V$ (as indicated in the text of Fig. 3.12). This voltage is in the linear

range (above $2V$), therefore the system responds adequately to changes in the load. At $U_3 < 2V$ shaft the hydraulic motor would not rotate independently of the load, which confirms that the two nonlinearities (overlapping of the distributor and the safety valve) are independent and must be taken into account when synthesizing regulators.

3. 2. 2 Transient processes in the closed system

3. 2.2.1 Transient processes in the closed system by assignment

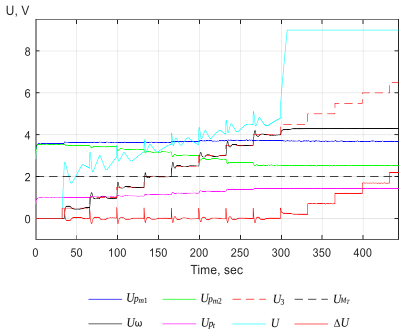

Fig. 3.23 Transient processes of a closed system when changing U_3 and under constant load $U_{M_T} = 1V$

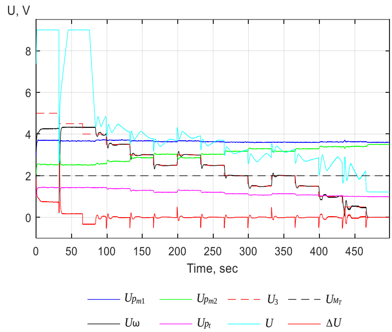

Fig. 3.24 Transient processes of a closed system when changing U_3 and under constant load $U_{M_T} = 1V$

Fig. 3.23 and Fig. 3.24 show a series of experimental transient processes in the tracking electrohydraulic system when changing the set voltage U_3 in the range from $0V$ to $7V$ with a step of $0.5V$ and a constant load voltage $U_{M_T} = 1V$. The following dependencies are observed on the graph:

- **Elimination of the dead zone:** In the open system (Fig. 3.6) the $U_3 < 1V$ валът на hydraulic motor does not rotate due to the positive overlap of the distributor. In the closed system, however, from U_3 $0V$ to $4.5V$, the shaft rotates with the corresponding angular velocity **from the smallest values** (Fig. 3.25). This is due to the integral component in the controller (*PID* or *Fuzzy-PID*), which compensates for the dead zone by increasing the control signal until the desired speed is reached.

- **Linear operating area:** In the range $0 – 4.5V$ the dependence $U_3 \rightarrow U_\omega$ is linear with high accuracy, thanks to the feedback.

- **Saturation zone:** At $U_3 > 4.5V$(up to $7V$) the speed does not change because the proportional valve is fully open – the same non-linearity as in the open system. The closed loop cannot overcome the physical limitation of the maximum flow rate.

- **Comparison with an open system:** In the closed system, the operating range is extended at the bottom ($0 – 4.5V$ instead of $2 – 4.5V$), and the accuracy is significantly higher (the established error tends to zero).

Fig. 3.26 shows a transient process with an increase in U_3 from $1.5V$ to $2V$ (100–150*s*), at constant load voltage $U_{M_T} = 1V$.

Fig. 3.27 presents transient processes with an increase in U_3 from $4V$ to $5.5V$ (period 300–360*s*), at a constant load voltage $U_{M_T} = 1V$. Due to the saturation of the proportional distributor at regulator voltages greater than $4.5V$, ($U > 4.5V$), the angular velocity of the hydraulic motor shaft does not change.

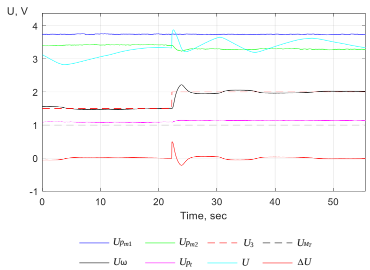

Fig.3.26 Transient processes of a closed system when U_3 changes and at constant load $U_{M_T} = 2V$ for the period of $100s$ up to $150s$

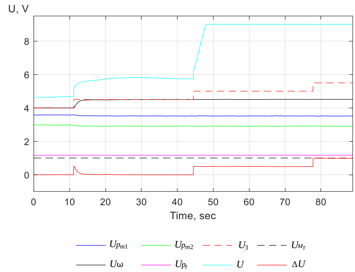

Fig.3.27 Transient processes of a closed system when U_3 changes and at constant load $U_{M_T} = 1V$ for the period of $260s$ up to $340s$

Conclusions :

1. The closed system eliminates the dead zone (0–2V) through the integral action of the regulator. This is a major advantage over the open system.

2. Dynamics are improved – shorter transition times and minimal overshoot.

3. Accuracy is significantly higher – the detected error is zero across the entire linear range.

Saturation above $4.5V$ remains a physical limitation – the closed loop cannot overcome it. It is necessary to limit the driving signals to $4.5V$ or to implement anti-windup strategies.

3. 2.2.2 Closed-loop system load transients

Fig. 3.28 shows a series of experimental transients in the tracking electrohydraulic system when changing the load voltage U_{M_T} in the range from $0V$ to $3V$ with a step of $1V$, at a constant command voltage $U_3 = 3V = const$.

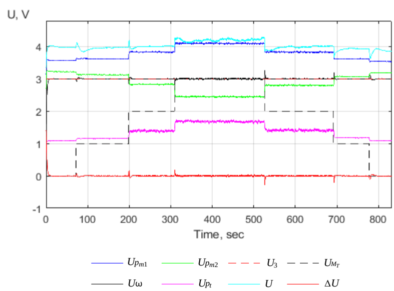

Fig.3.28 Transient processes of a closed system when changing the load U_{M_T} and constant tension $U_3 = 3V$

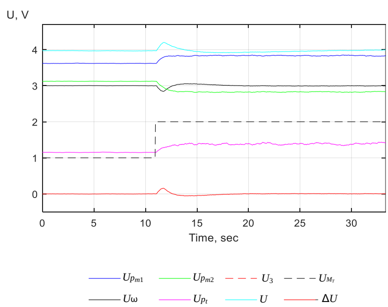

Fig.3.30 Transient processes of a closed system when changing the load U_{M_T} and constant tension $U_3 = 3V$ for the period from $170s$ to $200s$

When increasing the load voltage from $0V$ to $3V$, the angular velocity of the hydraulic motor shaft remains practically unchanged . The same applies to reducing the load from $3V$

to 0*V*. This is evidence of the effective operation of the closed loop - the *PI* controller compensates for the load disturbance by increasing the control signal to the proportional valve, maintaining the set speed. In the open system (Fig. 3.12) the same change in the load led to a significant decrease in speed (up to 30–40%). Here the error is reduced to almost zero in statics.

Fig. 3.30 shows a transient process at a constant input voltage, when the load voltage increases from 1*V* to 2*V* (period 170–200*s*).

Here the transition process is characterized by:

- **Larger disturbance** – load jump by 0.4*V* (from 1 to 2*V*).
- **Speed drop:** More noticeable – about 8–10% of the nominal value.
- **Recovery time:** Increases to approximately 2.7–3.2*s* because the regulator has to compensate for a larger deviation.
- **Transition shape:** Smooth decline followed by a monotonous increase to the set speed. No oscillations.
- **Conclusion:** The system successfully handles disturbances up to 2*V* , with the maximum dynamic deviation remaining within acceptable limits (below 10%).

Conclusions:

1. The closed system provides almost complete invariance to load disturbances – the static error is zero thanks to the integral component of the regulator.

2. The dynamic speed **deviation during a load jump is short-lived (2–3.5*s*)** and its amplitude increases with the magnitude of the disturbance, but remains within 15% for the studied range (0–3*V* load voltage).

3. The hysteresis characteristic of the open system is fully compensated – the response to increasing and decreasing load is symmetrical.

4. The quality of regulation (speed, accuracy, stability) is significantly higher compared to the open system, which justifies the use of a closed loop with an intelligent regulator (*Fuzzy-PID*).

5. Recommendation: For even better suppression of interference at large load jumps (above 3*V*), a more aggressive integral coefficient can be set, but with attention to stability. Experiments show that the current setting is stable and without overregulation.

CHAPTER IV

IDENTIFICATION OF THE PARAMETERS OF THE ELECTRO-HYDRAULIC TRACKING SYSTEM

4.1 Schematic diagram of the electro-hydraulic tracking system

Fig. 4.1 presents the schematic diagram of the automatic electro-hydraulic tracking system with a rotary actuator and a hydraulic loading subsystem, corresponding to the experimental setup in Fig. 4.1.

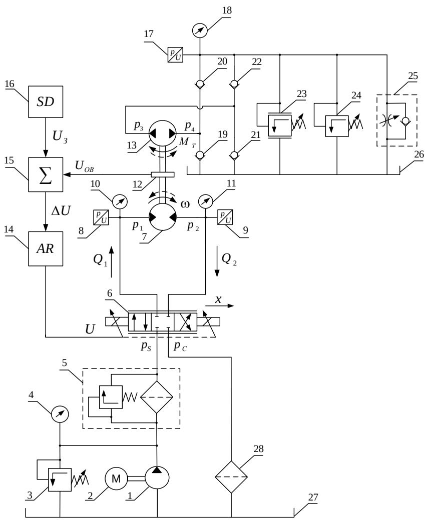

Fig. 4.1. Schematic diagram of the electrohydraulic tracking system

The elements of the electro-hydraulic tracking system are as follows:

1 – gear pump; 2 – electric motor; 3 – safety valve; 4 – pressure gauge; 5 – high-pressure filter with safety valve; 6 – proportional distributor ; 7 – hydraulic motor; 8, 9, 17 – pressure sensors; 10, 11, 18 – pressure gauges; 12 – speed sensor; 13 – gear pump (loading); 14 – automatic regulator; 15 – summing device; 16 – setting device; 19, 20, 21, 22 – check valves;

23 – proportional relief valve; 24 – relief valve; 25 – throttle with check valve; 26, 27 – tank; 28 – filter.

The system is powered by a hydro system including: oil tank 26; gear pump 1; safety valve 3; supply and discharge pipelines; pressure gauges 4 and 10; high-pressure filter with safety valve 5; low-pressure filter 28; proportional distributor 6; hydraulic motor 7.

Scheme operation

When the electric motor 2 is turned on, the pump 1 sucks working fluid from the tank 27. Along the pressure line, the fluid passes through a high-pressure filter with a safety valve 5 installed and reaches the inlet of the proportional distributor 6. The required pressure in the system is guaranteed by the settings of the safety valve 3, which is monitored by a pressure gauge 4. The hydraulic system is ready and awaits the supply of control voltage to the proportional distributor.

4.2 Modeling the hydraulic loading subsystem

4.2.1 Modeling a loading system using a proportional support valve

The case is considered when the proportional relief valve 23 is the loading element in the system Fig. 4.1. The adjustable throttle of the throttle with check valve 25 is fully closed, and the relief valve 24 is set to operate at a higher pressure. Fig. 4.2 shows a diagram of a loading system with a proportional relief valve. The pressure drop $\Delta p_{ППК}$ of the proportional relief valve can be written as:

$$\Delta p_{ППК} = p_t - p_a \approx p_t \tag{4.2}$$

$$p_t = \Delta p_{ППК_0} + k_{ППК} Q \tag{4.4}$$

Upon linearization of (4.4) and after transformation, the following equation is reached:

$$\Delta p_t = k_{U_T} \Delta U_T + k_{Q\,T} \Delta Q \tag{4.13}$$

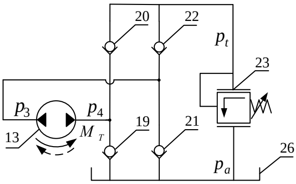

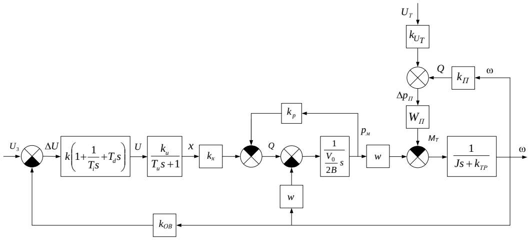

Fig. 4.2 Loading system with proportional relief valve

Fig. 4.4 . Structural diagram of a hydraulic monitoring system and a loading subsystem using a proportional relief valve

The structural diagram of the hydraulic system, using a loading system with a proportional relief valve, is presented in Fig. 4.4.

4.2.2. Modeling a loading system using an adjustable choke

We consider the case when the adjustable throttle of the throttle with check valve 25 is the loading element in the system in Fig. 4.4. When using the adjustable throttle of the throttle with check valve 25, the proportional relief valve 23 and the relief valve 24 are set to operate at a higher pressure.

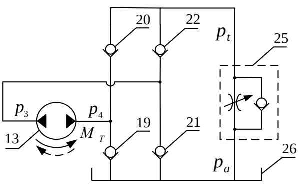

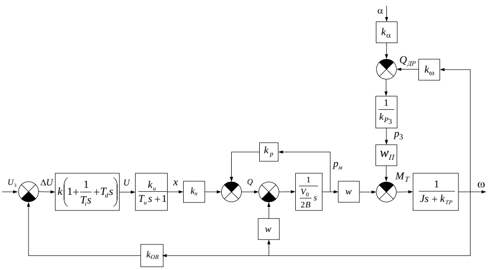

Fig.4.5 Loading system with throttle with check valve

Fig.4.6 Structural diagram of a hydraulic monitoring system and loading subsystem using an adjustable throttle

The flow rate through the throttle is expressed by the equation:

$$Q_{ДР} = \mu S_{ДР}(\alpha) 2 \sqrt{\frac{\Delta p_{ДР}}{\rho}} \tag{4.14}$$

The pressure drop across the throttle is expressed by the equation:

$$\Delta p_{ДР} = p_t - p_a \approx p_t \tag{4.15}$$

Upon linearization of (4.4) and after transformation, the following equation is reached:

$$\Delta Q_{ДР} = k_\alpha \Delta\alpha + k_{P_t} \Delta p_t \tag{4.19}$$

After transformation of (4.19), the pressure drop across the throttle is expressed as:

$$\Delta p_t = \frac{1}{k_{P_t}} \left(\Delta Q_{ДР} - k_\alpha \Delta\alpha \right) \tag{4.20 }$$

For the structural diagram of the hydraulic system, using a loading system with an adjustable throttle, we obtain:

4.3. Identification of the parameters of the electro-hydraulic tracking system

The identification of the parameters of the electrohydraulic tracking system (EHTS) is a key stage in the construction of an adequate mathematical model capable of describing with sufficient accuracy the dynamic behavior of the real object. The need for identification arises from the fact that some of the system parameters are difficult to measure, poorly known or subject to changes in the operation process.

The main goal of identification is to determine a vector of parameters so that the mathematical model of the system reproduces the experimentally observed processes with maximum accuracy.

$$\theta = \left[k_u, T_u, k_x, k_p, k_{\text{тр}}, J, k_{\text{ов}}, V_0\right]^T \tag{4.32}$$

The unknown parameters by which the identification of the rotary actuator system is performed are shown in Table 4.1:

Table 4.1. Unknown parameters

Parameter	Description	Units
$\boldsymbol{k_u}$	voltage gain	V/V
$\boldsymbol{T_u}$	time constant of the control element	s
$\boldsymbol{k_x}$	valve coefficient (flow/control)	m^2/s
$\boldsymbol{k_p}$	internal leakage coefficient	$m^3/(Pa \cdot s)$
$\boldsymbol{k_{\text{тр}}}$	viscous friction	$N \cdot m \cdot s$
$\boldsymbol{J}$	moment of inertia	$kg \cdot m^2$
$\boldsymbol{k_{\text{ов}}}$	feedback coefficient	$V \cdot s/rad$
$\boldsymbol{V_0}$	effective volume	m^3

4.3.1. Analysis of experimental data

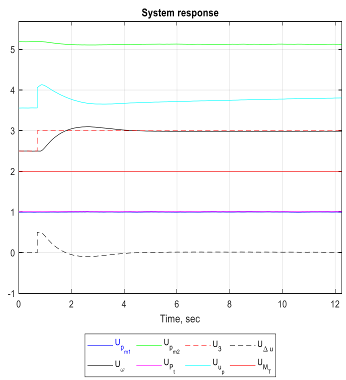

Fig. 4.7. Transient processes of the closed system when changing $\boldsymbol{U}_3$ and constant load $U_{M_T} = 2V$

Fig. 4.7 presents the experimentally obtained transient characteristics of the electrohydraulic tracking system with a step change in the input control input U_3 at a constant load. $U_{M_T} = 2V$

From the analysis of the obtained graphical dependencies, the following observations can be made:

- the system exhibits a clear overregulation;

- damped fluctuations are observed in the transient process;

- a final steady-state regime is established after a certain time.

4.3.6. Implementation of the identification procedure

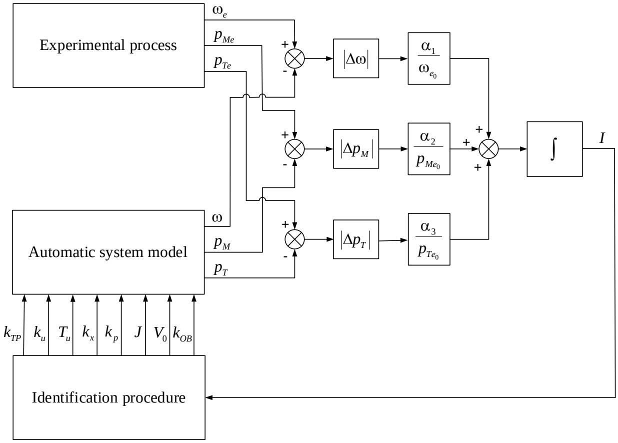

Fig.4.9 Scheme for performing the identification of the unknown parameters of the system.

The identification is implemented in the *MATLAB/Simulink environment* using the lsqnonlin function. The algorithm includes the following main steps:

- Setting initial values of parameters;
- Model simulation;
- Calculation of the error between model and experiment;
- Criterion minimization;
- Update of parameters;
- Iterate to convergence.

Fig. 4.9 presents a scheme for parameter identification. The experimental characteristics of the real system are introduced as a basis for comparison. The difference (error) between the experimental results and the results of the model of the automatic system is determined. To determine the values of the tuning parameters of the automatic system, an identification procedure has been developed in *MATLAB/Simulink* , which is based on the nonlinear least squares optimization method (Levenberg–Marquardt algorithm, lsqnonlin function). It defines the integral proximity criterion I, by performing minimization with respect to the evaluated parameters by changing the model parameters.

4.3.7. Identification results

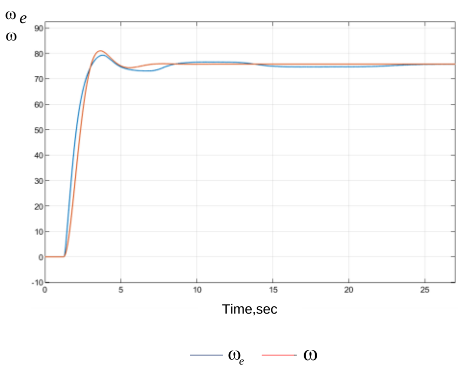

Fig.4.10 Transient processes during rotation of the hydraulic motor shaft, change in angular velocity

Fig. 4.10 shows the transient processes when changing the angular velocity of rotation of the hydraulic motor shaft from the experimental process ω_e and the one after identification.

The identification results are presented in Table 4.1. In the identification process, constraints on the parameters were introduced to ensure physical feasibility and avoid numerical instability. The limits were selected based on a priori engineering information about the system and typical parameter values in electro-hydraulic drives.

Table 4.7 Identification results

Parameters	k_u U/m	T_u s	k_x m^2/s	k_p $m^3/Pa.s$	$k_{тр}$ $kg.m^2/s$	J $kg.m^2$	$k_{ов}$ $V.s/rad$	V_0, m^3	I –
Initial values	5.000x10 $^{-4}$	0.2000	0.7500	9.545x10 $^{-10}$	0.2000	1.000x10 $^{-4}$	0.1200	4.477x10 $^{-5}$	41,760
End values	8.561x10 $^{-4}$	0.5905	0.7576	2.673x10 $^{-9}$	0.0189	1.095x10 $^{-5}$	0.0528	4.425x10 $^{-5}$	1.016
Limits (boundaries)	[10 $^{-5}$ ÷ 10 $^{-3}$]	[0.05 ÷ 1]	[0.1 ÷ 1.5]	[10 $^{-10}$ ÷10 $^{-8}$]	[0.001 ÷ 1]	[10 $^{-6}$ ÷ 10 $^{-3}$]	[0.01 ÷ 0.2]	[10 $^{-6}$ ÷ 10 $^{-4}$]	–
Relative change (%)	+71.22%	+195.25%	+1.01%	+180.09%	−90.55%	−89.05%	−56.00%	−1.16%	−97.57%

The table shows that the most significant changes are observed in the parameters $T_u, k_p, k_{тр}$and J, which indicates their dominant influence on the dynamics of the system. A relatively small change in $k_x$and V_0indicates a lower sensitivity of the model to these parameters. The significant reduction of the integral criterion $I$by over 97% confirms the effectiveness of the identification procedure.

Analysis of results

The analysis conducted shows a clear distinction between the parameters by degree of influence:

- Critical parameters (very high sensitivity):

T_u, k_p, $k_{тр}$, J→ determine the basic dynamics (inertia, friction, hydraulics)

- Significant parameters (high sensitivity):

k_u, $k_{ов}$→ affect amplification and stability

- Weakly sensitive parameters:

k_x, V_0→ have limited influence on transients

Sensitivity analysis shows that the dynamic behavior of the electrohydraulic tracking system is determined to a large extent by the parameters related to the inertial, dissipative and hydraulic properties of the system. This allows for a reduction of the model by fixing the weakly sensitive parameters and concentrating the identification procedure on the dominant parameters, which leads to improved numerical robustness and faster convergence of the optimization algorithm.

CHAPTER V

DESIGN OF INTELLIGENT CONTROL FOR ELECTROHYDRAULIC TRACKING SYSTEM

5.1. Designing a *Fuzzy* Controller

5.1.1. Fuzzy control structure

Fuzzy *Logic Controllers* use the principles of fuzzy logic to mimic expert decision-making and control. These types of controllers are particularly suitable for controlling systems whose mathematical models are imprecise, incomplete, or too complex. Instead of precise models, they use expert knowledge and linguistic rules.

Therefore, the study of fuzzy control and its comparison with traditional *PID* control and typical control laws is of great importance for modern control theory. Fuzzy logic control uses methods in the form of rules to control a given process. A *fuzzy* logic controller can have an unlimited number of input signals and is built on the basis of expert knowledge.

The goal is to expand the possibilities for upgrading *PID* controllers, which occupy a basic level in the hierarchy of control systems. Therefore, the design of fuzzy *PID* controllers can be considered as an optimization problem, the solution of which determines the optimal values of the tuning parameters. Modern trends in the control of automated systems are aimed at implementing hybrid systems, combining more than one control technique.

The rule base consists of a set of predefined logical rules of the "*if–then*" type, which describe the control strategy and are obtained based on expert knowledge. The value of the output quantity (u) in fuzzy control is determined by rules of the type:

$$Rn: if\ e\ is\ Ai\ and\ \Delta e\ is\ Bi\ then\ k\ is\ Ci$$

where e, Δe, k, $T_i$and $T_d$are linguistic variables corresponding to the input-output quantities. Their universal sets are determined by the ranges of variation of the corresponding quantities:

$$[-e, e], [-\Delta e, \Delta e], [-k, k], [-T_i, T_i] и [-T_d, T_d].$$

The sets A_i, $B_i$and $C_i$are fuzzy sets, uniformly distributed in these ranges. In the fuzzification process, the input data is converted from numerical values to linguistic variables. Then, the rules from the knowledge base are applied. In the defuzzification process, the resulting result is converted back to a numerical value, which is used as a control effect on the object.

Fig. 5.1 shows a schematic diagram of an electrohydraulic tracking system with a rotary actuator and parallel *Fuzzy* and *PID* controllers.

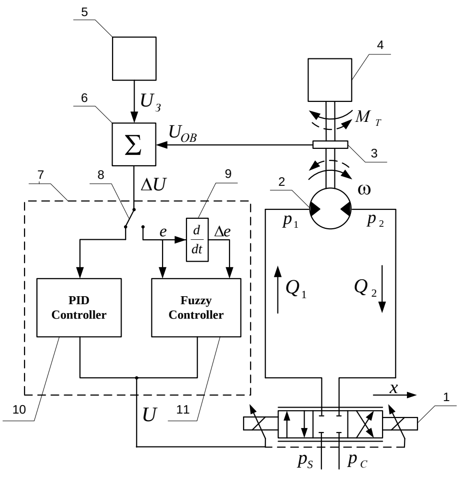

Fig.5.1 Schematic diagram of an electrohydraulic tracking system with parallel connected Fuzzy and *PID* controllers

The system consists of the following elements: 1 – proportional valve; 2 – hydraulic motor; 3 – shaft speed sensor; 4 – regulated object; 5 – personal computer supplying a set voltage; 6 – summing device; 7 – electronic control unit consisting of parallel connected *Fuzzy* and *PID* regulators; 8 – control switch; 9 – integrating unit; 10 – *PID* regulator; 11 – *Fuzzy* regulator.

The hydraulic tracking system can be controlled with both *PID* and *Fuzzy* controllers by switching the control switch.

The fuzzy output mechanism in the logic block determines the decision for the parameters of *the PID* controller. The Mamdani max-min composition method is used:

$$\mu_i = max(min[\mu_{Aj}, \mu_{Bk}]) \qquad (5.1)$$

where: μ_{Aj} and μ_{Bk} are degrees of superposition.

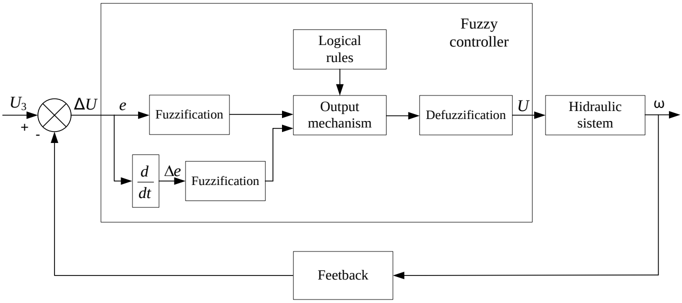

Fig.5.2 The structural diagram of the automatic electrohydraulic system with a fuzzy controller

In the defuzzification block, the transition from fuzzy to real values of the output quantities k , T_i and T_d is implemented using the center of gravity method in the form:

$$k_0 = \frac{\sum_{i=1}^{m} k_i \mu(k_i)}{\sum_{i=1}^{m} \mu(k_i)} \qquad (5.1)$$

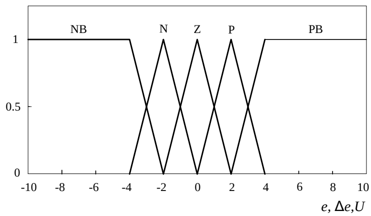

Fig.5.3 Membership functions of the input-output quantities *e, Δe , U*

where k_i are the centers of the activated fuzzy sets, and $\mu(k_i)$ are the degrees of membership in them.

Each input and output is described by a set of terms: *Negative Big* (NB) *Negative* (N), *Zero* (Z), *Positive* (P) , *Positive Big* (PB) . Fig. 5.3 presents the membership functions of the input-output quantities – *e*, Δ *e*, and *U*. The rules that build the logic of the fuzzy controller are presented in Table 5.1.

Table 5.1 The rules that build the logic of the fuzzy regulator

Δ is / ***yes***	***NB***	***N***	***Z***	***P***	***PB***
NB	*NB*	*NB*	*N*	*N*	*Z*
N	*NB*	*N*	*N*	*Z*	*P*
Z	*N*	*N*	*Z*	*P*	*P*
P	*N*	*Z*	*P*	*P*	*PB*
PB	*Z*	*P*	*P*	*PB*	*PB*

Figure 5.4 presents the three-dimensional model of the fuzzy controller.

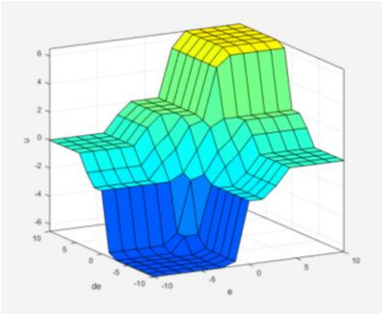

Fig.5.4 Three-dimensional model of the fuzzy controller

Figure 5.5 shows the transient processes in the automatic system when changing the input value, the reference voltage U_3 , the disturbing voltage U_{M_T} when using *Fuzzy* and *PID* controller. In the figure they are marked as follows: $U_{\omega\,FUZZY}$ - voltage of the angular velocity sensor when using *Fuzzy* controller; $U_{\omega\,PID}$ - angular velocity sensor voltage when using *PID* controller; U_3 - reference voltage; U_{M_T} - load voltage.

From Figure 5.5 it can be seen that the use of *Fuzzy* controller leads to a significant reduction in the duration and overregulation of the transient processes occurring in the system.

Figure 5.6 compares the output voltage transients using *Fuzzy* and *PID* controller. The difference in the behavior of the two controller is clearly observed. The use of *Fuzzy in the system* controller is associated with a sharp change in its output value in the range of -5*V* to +5*V*. In the established mode, the output values of the two controller coincide. The figure shows: U_{FUZZY} - voltage at the output of *Fuzzy* the controller; U_{PID} *PID* output voltage the controller .

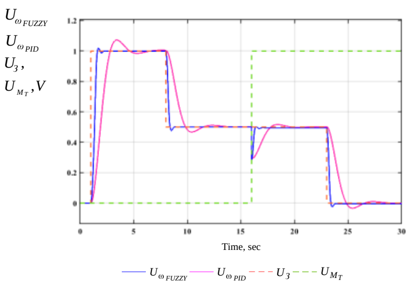

Fig.5.5 Change in output values in the *Fuzzy* and *PID* controller of the tracking system

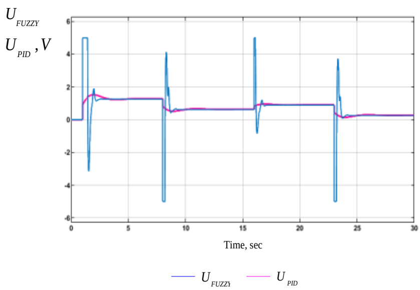

Fig.5.6 Voltage at the output of *Fuzzy* and *PID* controllers

5.1.2. Investigating the real system with FUZZY controller

To synthesize a *FUZZY* controller with two input terms, a method [116] is used to design a class of fuzzy controllers, based on obtaining analytical expressions for the control effect of the output of the fuzzy controller under symmetric triangular influences. A methodology is presented, based on which a fuzzy controller based on a *PI* controller is synthesized. For simplicity, we will choose a value for N = 2, where N is the number of subsets of the output. As membership functions, we choose Λ-terms. The degree of membership is obtained by calculating the *fuzzy* membership value of a given function for the corresponding speed. The basic rules are shown in Fig. 5.9.

		Error	
speed		P	N
	P	P	Z
	N	Z	N

Fig. 5.9. Basic rules for fuzzy control with two input terms

After determining all the parameters of the fuzzy controller, we set the data in the Simulink model of Fig. 5.10 . The results of the study showed that the designed fuzzy controller does not fully meet the regulation time requirement ($t_s > 3s$). This is due to its low accuracy. This problem was solved by slightly adjusting the coefficient G_o by about a quarter, to the value $G_o = 0.05$.

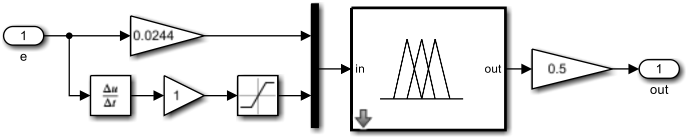

Fig. 5.1 0 Simulation model of *a FUZZY* controller with two input terms

In order to improve the quality of regulation, a single-loop system with a fuzzy controller and an additional speed input has been synthesized. The controller includes three input variables – error (*error*), rate of change of the error ($speed_e$) and motor speed ($speed_v$), and one output variable ($output$) (Fig. 5.13).

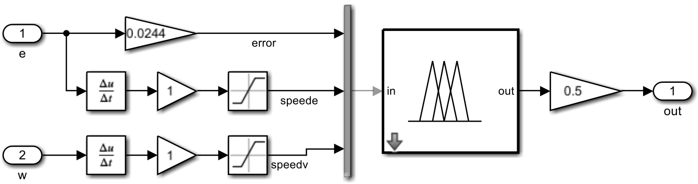

Fig. 5.13 Simulation model of *a FUZZY* controller with three input terms

Five *fuzzy* terms are defined for the input variables: *Large negative* (BN), *Medium negative* (MN), Zero (Z), *Medium positive* (MP), and *Large positive* (LP). Symmetric triangular membership functions are used, and defuzzification is implemented using the center of gravity method.

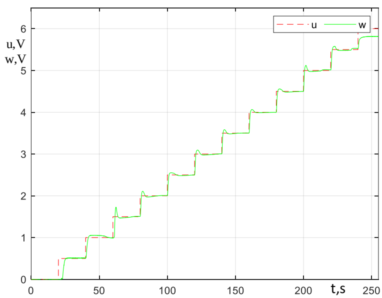

Fig. 5.12. Reaction of the system with a fuzzy controller I to a change in the setpoint

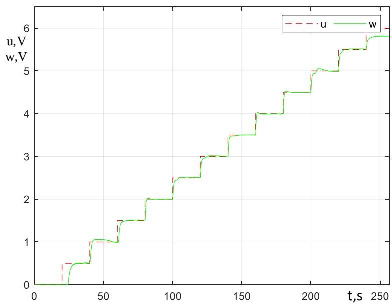

Fig. 5.15 Reaction of the system with fuzzy controller II to a change in the setpoint

The angular velocity of the motor is used as an additional correction parameter. When it is within the specified range, the control action is determined by the error and its rate of change, without additional restrictions.

Table 5.5 compares the main quality indicators of the system with the three controller. The operating control range is divided into three intervals: 0 ≤2.5, (2.5,4] and ≥4.5. When the system is loaded, the best indicators are obtained in the middle range.

Table 5.5 . Direct qualitative indicators of transient processes.

	range	**System with PI controller**		**Fuzzy controller system I**		**Fuzzy Controller System II**	
		minutes	**max**	**minutes**	**max**	**minutes**	**max**
Overshoot, σ(%)	≤2.5	2	11.6	0	16	0	5
	(2.5,4]	0	1.63	1.5	3.3	0	0.75
	≥4.5	0	2.89	1.33	2.8	0	1
Transient duration, ts (s)	≤2.5	6	12	7	16	4	10
	(2.5,4]	6	10	4	10	4	8

Thus, we obtained the minimum overshoot when using a *fuzzy* controller II, the maximum overshoot when using a *PI* controller. The use of the *PI* controller also leads to the appearance of oscillations in the system, which can significantly worsen the quality of the drive, and in this case (due to a large overshoot) can even lead to equipment damage and an accident.

The system with *PI* controller has maximum transient time and to find the transient time for *PI* controller, it was necessary to increase the time interval under consideration. The transient time is minimum when using *fuzzy* controller II. If we consider direct quality indicators, then the most effective is fuzzy controller II.

5.2 Designing an adaptive *Fuzzy* - *PID* controller

The adaptive *fuzzy PID* controller is a type of intelligent controller that combines the principles of *fuzzy* logic with those of adaptive control . This combination allows it not only to use linguistic rules and expert knowledge to control systems like a standard *fuzzy* controller, but also to change its parameters or rules in real time in response to changes in the controlled object, external disturbances, or changing operating conditions.

The advantages of the adaptive *fuzzy* controller are that it is effective in controlling complex nonlinear systems and the ability to maintain high performance even when the characteristics of the object change significantly .*PID* operation

The regulator can be described in two ways with the equations:

$$u = k\Delta u + k_i \int \Delta u dt + k_d \frac{d\Delta u}{dt} \tag{5.13}$$

where : $k_i = \frac{k}{T_i}$, $k_d = kT_d$.

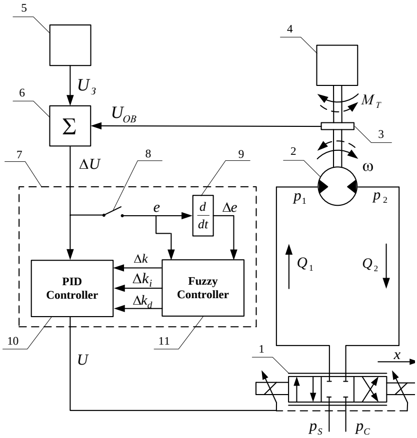

Fig.5.16 Schematic diagram of an adaptive fuzzy *PID* controller

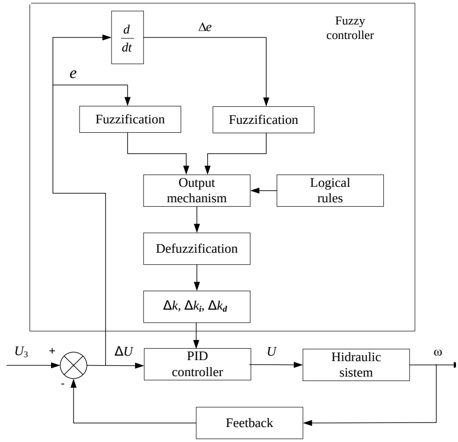

Fig.5.17 The structural diagram of the automatic electrohydraulic system with a fuzzy controller

Fig.5.16. shows a schematic diagram of an electrohydraulic tracking system with a rotary actuator. The system consists of the following elements: 1 – proportional valve; 2 – hydraulic motor; 3 – speed sensor of the hydraulic motor shaft; 4 – control object; 5 – personal computer supplying a set voltage; 6 – summing device; 7 – automatic adaptive controller, consisting of two parts – *PID* controller and *Fuzzy* controller; 8 – control switch; 9 – integrating unit; 10 – *PID* controller; 11 – *Fuzzy* controller. Depending on the position of switch 8, the hydraulic monitoring system can be controlled in two ways - with *a PID* controller and with an adaptive *PID* controller with variable coefficients, which are output values of *Fuzzy* the controller.

A structural diagram of the automatic electrohydraulic system with the developed fuzzy adaptive *PID* controller is shown in Fig. 5.17.

Fig. 5.18 shows a diagram describing the operation of the adaptive *PID* controller.

The coefficients – k, k_i and k_d, are obtained after summing the initial *PID settings.* the controller - k_0, k_{i0} and k_{d0} and the adaptive add-ons from *Fuzzy* the regulator - Δk, Δk_i and Δk_d:

$$k = k_0 + \Delta k \tag{5.15}$$

$$k_i = k_{i0} + \Delta k_i \tag{5.16}$$

$$k_d = k_{d0} + \Delta k_d \tag{5.17}$$

where: k_0, k_{i0} and k_{d0} - initial settings of *PID* parameters the controller;

Δk, Δk_i and - Δk_d *fuzzy* output values the controller.

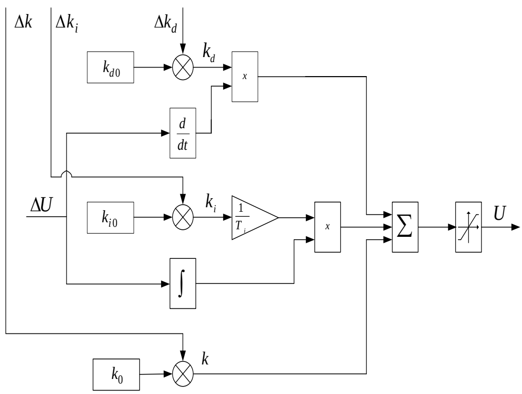

Fig.5.18 Adaptive *PID* operation diagram controller

Fig. 5.20 and Fig. 5.21 present the membership functions of the fuzzy sets of the input *e*, Δ*e* and the output quantities Δ*k*, ΔT_i *and* ΔT_d.

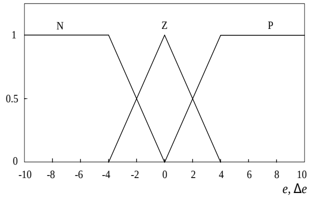

Fig. 5.20 Membership functions of the input quantities *e* and Δ*e*

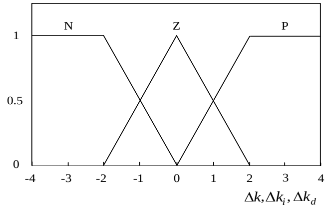

Fig. 5.21 Membership functions of the output quantities Δ*k*, Δ k_i and Δ k_d

Each input and output is described by a set of terms: *Negative* (N) , *Zero* (Z), *Positive* (P) . The rules that build the logic of the fuzzy controller are shown in Table 5.2, Table 5.3 and Table 5.4. They are formulated based on expert knowledge about the behavior of the *PID* controller:

Table 5.6 The rules of the fuzzy controller for Δk

Δ is / ***yes***	***N***	***Z***	***P***
N	*P*	*P*	*Z*
Z	*N*	*P*	*P*
P	*Z*	*N*	*N*

Table 5.7 The rules of the fuzzy controller for Δ k_i

Δ is / ***yes***	***N***	***Z***	***P***
N	*P*	*P*	*Z*
Z	*N*	*P*	*P*
P	*Z*	*P*	*P*

Table 5.8 The rules of the fuzzy controller for Δ k_d

Δ is / ***yes***	***N***	***Z***	***P***
N	*N*	*N*	*Z*
Z	*P*	*Z*	*P*
P	*Z*	*N*	*N*

The three-dimensional models in Fig. 5.22, 5.23 and 5.24 illustrate the nonlinear dependence of Δk, $\Delta k_i$and Δk_d on e and Δe. It can be seen that the surfaces are smooth and without sharp jumps, which guarantees a stable change in the parameters of *the PID* controller during operation. This allows the adaptive *Fuzzy -PID* controller to adjust automatically in different modes – for example, during start-up, stop or sudden disturbance.

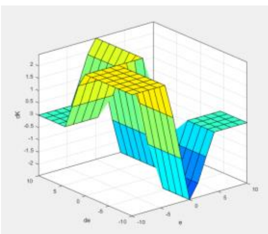

Fig. 5.22 Three-dimensional model of Δ*k*

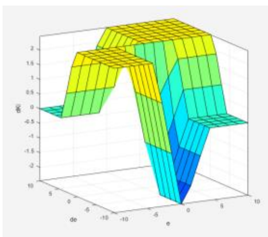

Fig. 5.23 Three-dimensional model of Δk_i

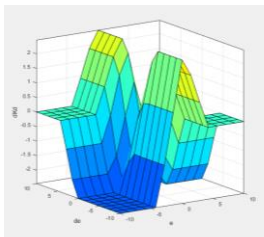

Fig. 5.24 Three-dimensional model of Δk_d

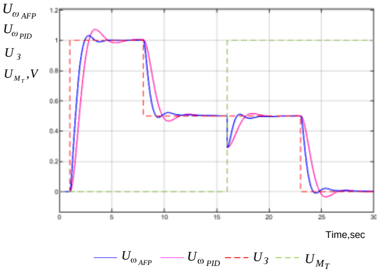

Fig.5.25 Change of output values in *Fuzzy* and *PID* the tracking system controller

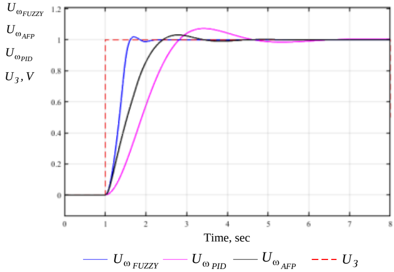

Fig.5.26 Change of output values in *Fuzzy* , adaptive *Fuzzy PID* and *PID* the tracking system controller

Fig. 5.25 presents the transient processes in the automatic electrohydraulic tracking system when changing the input value – the setpoint voltage and the disturbance voltage when using *PID* and adaptive fuzzy *PID* controllers. The presence of overregulation when changing the setpoint is inevitable due to the dynamic properties of the electrohydraulic system, but when using an adaptive fuzzy *PID* controller it is significantly limited and well damped, which leads to a higher quality of control compared to the classic *PID* controller.

Fig. 5.26 compares the transient processes occurring in the automated system using a fuzzy controller, an adaptive fuzzy *PID* controller and *PID* controller.

5.3 Experimental studies of the automatic electrohydraulic tracking system with *Fuzzy PID* controller

5.3.1. Matlab Simulink model for control of the EHTS

In fig. 5.27 shows the *Matlab Simulink* model of the implemented real-time control of an electro-hydraulic tracking system.

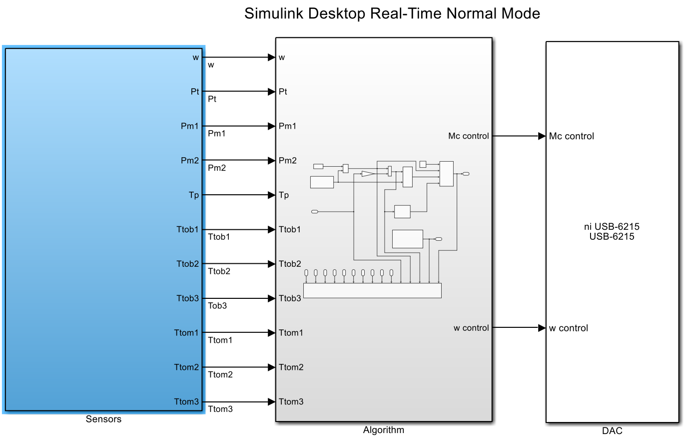

Fig. 5.27. Matlab Simulink model for real-time control of an electrohydraulic tracking system

The connection with the sensors on the stand and reading of the data from them is performed by the Sensor subsystem, and the control of the servo valve by the DAC subsystem. The measured data from the sensors are filtered in real time by a lowpass filter of Butterworth with the following settings Filter Order = 1 and Passband edge frequency = 0.05 rad/s. The data thus obtained are fed to the Algorithm module, where the adaptive *Fuzzy-PID* controller is implemented Fig. 5.28.

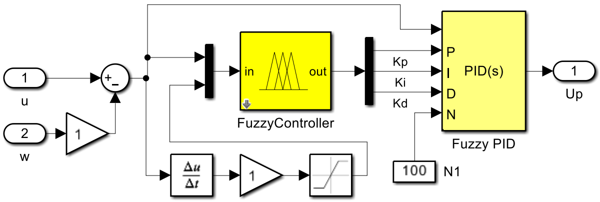

Fig. 5.28. Simulation model of control with an adaptive fuzzy *PID* controller

The input of the regulators is supplied U_3(reference voltage) in volts ($1{,}0\,V \cong 150$). The regulators also generate output values in volts. These values are supplied through a digital-to-analog converter (DAC) to the proportional valve of the hydraulic system and drive the hydraulic motor. All signals returned by the sensors are visualized in volts. Three pressures and the voltage (revolutions) returned by the tachogenerator are monitored.

5.3.2 Transitions of the ECS on assignment

Fig. 5. 29 presents transient processes of the real electrohydraulic tracking system with integrated *Fuzzy PID* with step change of the reference voltage U_3, and constant load voltage $U_{M_t} = 1V$ with the throttling gap corresponding to the screw rotation angle $\alpha = \pi/4$.

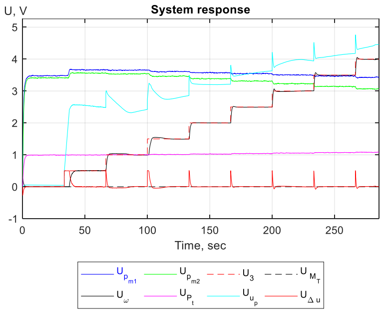

Fig. 5.29 Transition processes of the EHTS when changing the task U_3in an increasing direction

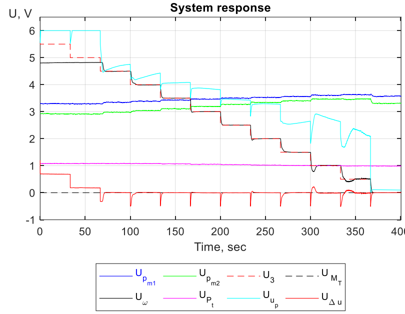

Fig. 5.30 Transitional processes of the EHTS when changing the task U_3in a decreasing direction

In this operating mode, the setpoint changes from 0 to $5V$. The setpoint increment step is $U_3 = 1V(\cong 150\,rpm)$, and the hold time is 50s . The transient process implemented with *Fuzzy PID* controller, shows a rapid increase in the output value without visible overregulation. The regulation time is less than 1.5s, and the static error in a steady state is zero. The absence of oscillations is due to the ability of *Fuzzy* The regulator limits overshoot by nonlinearly varying the control signal. The throttling gap, fixed by angle α_1, introduces some damping that does not degrade stability.

At a setting of $1.5V$ ($\cong 230\,rpm$), overshoot is observed $\sigma = 3\%$, and the duration of the transient process is $t_p = 7\,sec$.

At a setpoint of $2.5V$ ($\cong 380\ rpm$) there is no overshoot, with a duration of the transient process$t_p = 2.3\ sec$

At a setpoint of 4V ($\cong 600\ rpm$), the overregulation is $\sigma = 0.67\%$, at a duration of the transient process. $t_p = 2.59s$.At all sets, a time delay in the system response of the order of $\tau = 0.2s$. The dynamics of the system are similar when the setpoint is reduced (Fig. 5.30)

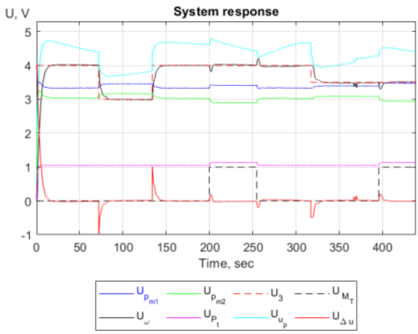

Fig. 5.31 Transient processes of the EHTS during load changes

5.3.3 Transients of the EHTS by disturbance U_{M_t}

Fig. 5.31 presents transient processes of the electrohydraulic tracking system during stepwise changes in the load voltage U_{M_t}, at a constant set voltage $U_3 = 2V$and the throttling gap corresponding to the screw rotation angle $\alpha = \pi/4$.

When loading and unloading by 20% ($U_{M_t} = 1V$ and $U_3 = 1V$) the system settles for a time $t_p \cong 7.6\ sec$. The system speed changes by a maximum of $0.19V$ which is equivalent to 28 rpm. No increase in revolutions above the set value is observed.

5.4. Synthesis of a robust control device

The synthesis of the robust control is based on the mathematical model of the system described by the differential equations 5.5–5.7. Due to the nonlinear nature of the model, it is not suitable for direct H_∞ synthesis using the methods presented in [1,2]. Therefore, linearization around the operating point is performed, where the nonlinear system is replaced by an equivalent linear model described by equations (5.18).

$$
\begin{aligned}
&J\dot{\omega} = wp_M - k_{TP}\omega - M_T \\
&\dot{Q} = \frac{K_{x_0}}{T_u}(K_u u - x) - \frac{2BK_p}{V_0}(Q - w\omega) \\
&\frac{V_0}{2B}\dot{p_M} = Q - w\omega \\
&T_u\dot{x} = k_u u - x
\end{aligned}
\tag{5.18}
$$

The synthesis of the robust control is based on the mathematical model of the system described by the differential equations 5.5–5.7. Due to the nonlinear nature of the model, it is not suitable for direct H_∞ synthesis using the methods presented in [1,2]. Therefore, linearization around the operating point is performed, where the nonlinear system is replaced by an equivalent linear model described by equations 5.18.

In modeling, some of the parameters can be determined with high accuracy through preliminary studies, analytical evaluation of volume losses and the volumetric efficiency coefficient [8]. Other parameters, such as $J, K_u и T_u$, are assumed to be undetermined within predefined limits.

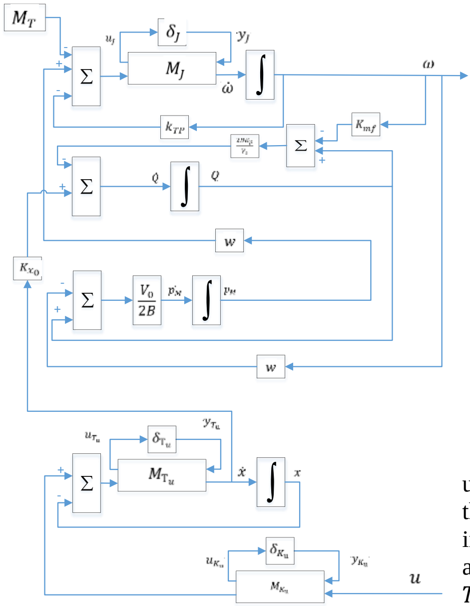

Fig. 5. 3 2. Block diagram of the mathematical model of the system

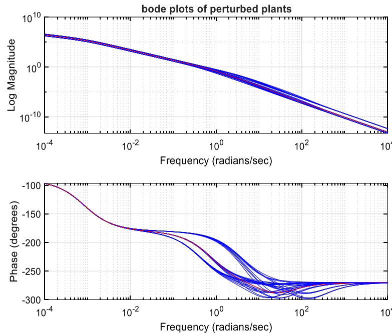

Fig. 5. 3 3 The amplitude-frequency and amplitude-phase characteristics of the disturbed open system.

The following parametric uncertainties were taken into account in the synthesis: 30% for the moment of inertia J, 50% for the gain coefficient K_u, and 30% for the servo valve time constant T_u.

The nominal values of the parameters are indicated by$\bar{J}$, $\overline{K_u}$and $\overline{T_u}$. The block diagram of the system is presented in Fig. 5.32.

The inputs of the system are the uncertainties w, disturbances $d$and the control effect u, and the outputs are the uncertainties, errors and measurements. The goal of the synthesis is to find a controller K that provides internal stability and minimizes the influence of disturbances on the error in the sense of H_∞ the -norm for all admissible uncertainties.

To increase robustness, a H_∞synthesis problem with a nominal quality requirement has been solved.

$$\left|W_p I + GK^{-1}\right|_\infty < 1 \tag{5.28}$$

where $I + GK^{-1}$is the sensitive function of the closed system.

The synthesis was implemented in *MATLAB* by calculating a suboptimal H_∞controller. With a selected interval $[1; 2.10^{10}]$ and tolerance of 0.01 γ, a fifth-order controller was obtained, but with a norm greater than 1, which is why the quality condition is not met.

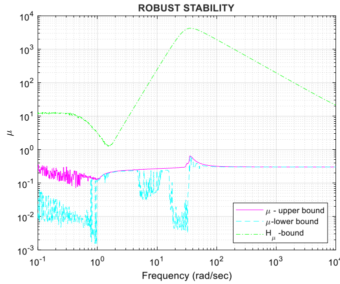

Fig.5. 3 4 Robust stability of the closed system with K_{H_∞}

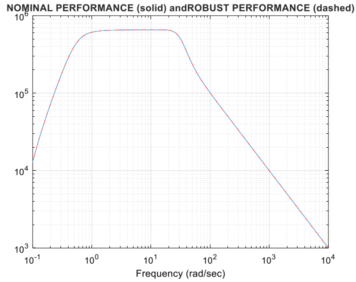

Fig.5.35. Nominal (-) and stable (--) performance for K_{H_∞}

The robustness is assessed by the structured singular number μ. From the frequency characteristics Fig. 5.34 it is established that the system is robustly stable, with the maximum value being $\mu = 0.64957$. The analysis of the nominal and robust quality shows that the system with H_∞ a controller satisfies the set requirements.

Fig. 5.36 shows the simulated transients at the setpoint with the resulting H_∞controller, and Fig. 5.37 – under disturbance.

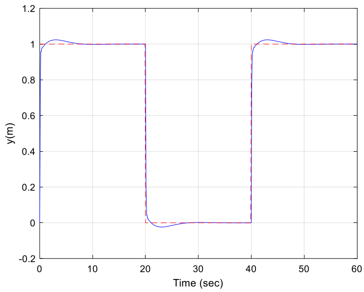

Fig.5.36 Transient processes of a closed system withK_{H_∞}

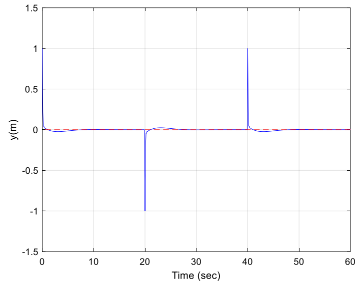

Fig. 5.37. Transient processes in the event of a disturbance in the closed system withK_{H_∞}

Performing H_∞ synthesis only on the output sensitivity provides good transients and a lower order of the regulator, but leads to unacceptable values of the control signal. Therefore, (H_\infty) synthesis with minimization of the mixed sensitivity criterion was chosen, which allows limiting the control impact and the required control energy.

Using weight matrices: $W_1(s) = \frac{0.01}{s+2.5}$, и $W_2(s) = \frac{0.77s}{1.4s+0.001}$, implementing a low-pass and high-pass filter, respectively, a sixth-order controller is synthesized. The resulting closed-loop system is robustly resistant to object uncertainties and provides both nominal and robust control quality (Fig. 5.38 and Fig. 5.39).

The transient processes at the setpoint and in the event of a disturbance are presented in Fig. 5.40 and Fig. 5.41. The resulting regulator provides a technically acceptable transient process and a control signal within acceptable limits.

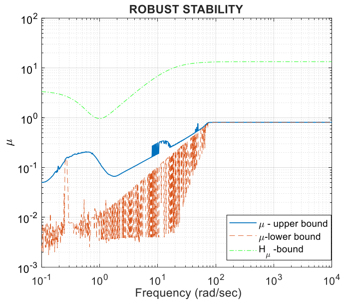

Fig. 5.38. Robust closed-loop system stability with the second K_{H_∞} controller.

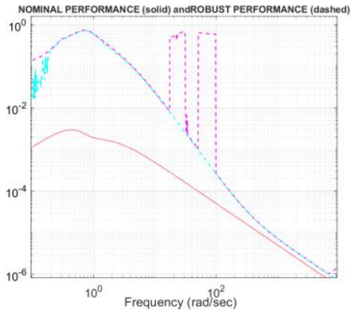

Fig. 5.39. Nominal (-) and robust (--) control quality for the second K_{H_∞}controller.

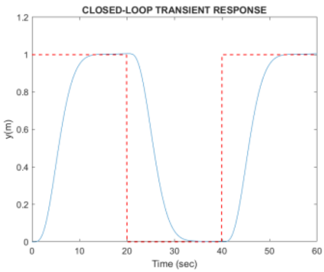

Fig.5.40 Transient processes of the closed system with the secondK_{H_∞}

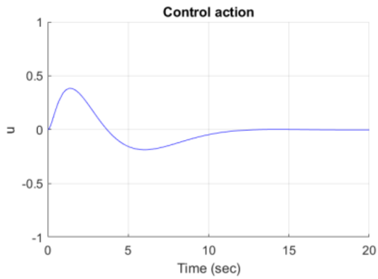

Fig. 5.41. Transient processes upon disturbance of the closed system with the secondK_{H_∞}

5.5. Conclusions to Chapter V

The chapter explores the possibilities of applying modern methods for controlling an electro-hydraulic tracking system (EHTS). Through analysis, simulations and experimental studies, classical *PI/PID* , fuzzy , adaptive *Fuzzy PID* and robust H_∞ controllers have been developed and compared.

Main contributions and results:

1. **The analysis of *PI* control** shows a significant dependence of the dynamic characteristics on the operating point. The settling time is in the range of 2–13s, and the overshoot reaches 11.6%, which confirms the limited robustness of linear regulators.
2. **The designed *Fuzzy* controller** provides a significant improvement in control quality with a settling time of about 1.2s and overshoot below 2%, outperforming *PI* and *PID* controllers.
3. **The developed adaptive *Fuzzy PID* controller** changes the parameters k, $k_i$and in real time according to the error and its change. The indicators k_d and $\sigma < 4\%$were obtained $t_s \approx 2{,}2s$, which is an improvement over the classic *PID* controller.
4. **Experimental studies of the real system** with *Fuzzy PID* controller is confirmed by simulation studies. When changing the setpoint from 0 to 5*V*, the system demonstrates a fast transient process and minimal overshoot, and at a 20% disturbance it restores the established mode without overshoot.

5. **A robust H_∞controller** based on a linearized model with parametric uncertainties (30% for the moment of inertia, 50% for the gain, 30% for the servo valve time constant) has been synthesized. Through μ-analysis, it has been proven that the closed-loop system is robustly stable (maximum value of μ=0.65). The transients with the H_∞ controller have a duration of about 6.5 s and an overshoot of about 4%, which is comparable to PI, but with better stability under disturbances.
6. **controller** based on a linearized model with parametric uncertainties $\mu -$ анализhas been synthesized . Through H_∞ the robust stability of the system $\mu_{max} = 0{,}65$, the resulting transients have a duration of about 6.5s and an overshoot of about 4%, ensuring higher resistance to parametric changes and disturbances.

A summarized analysis of the regulators is shown in Table 5.11.

Table 5.11 : Comparative analysis of controller:

Regulator	ts	σ	Robustness	Complexity	Adaptability	Resistance to nonlinearities
PI/ *PID*	3.3–13 seconds	0–11.6%	low	low	missing	low
Fuzzy	1.2 seconds	<2%	high	average	partial	high
Fuzzy -PID	2.2 seconds	<4%	very high	high	high	very high
H $_\infty$	6.5 seconds	≈4%	robust	high	limited	average

General conclusions:

- **The best dynamic performance** is provided by the pure *Fuzzy* controller, but the price is aggressive control impact (up to ±5*V*) and higher requirements for the actuators.
- **The adaptive *Fuzzy -PID* controller** represents an optimal compromise between speed, smoothness and robustness. It is most suitable for real industrial applications where there are restrictions on the control signal and reliability is required under changing parameters of the object.
- **The robust H∞ controller** guarantees robustness under significant parametric uncertainties, but is inferior to intelligent methods in terms of speed of response. It is recommended for systems where safety and guaranteed stability are critical.

CONTRIBUTIONS OF THE DISSERTATION

Scientific and applied contributions

1. A nonlinear and linearized mathematical model of an automated electrohydraulic tracking system with a rotary actuator, which takes into account the basic physical processes and the nonlinearity of the object, has been developed and studied. The behavior of the system in different operating modes has been studied.

2. A methodology with software implementation for parametric identification of an electrohydraulic tracking system has been developed , based on experimental data, applicable to different types of loading subsystems and allowing for increasing the adequacy of the mathematical model in the presence of nonlinearities.

3. *Fuzzy*, adaptive *Fuzzy–PID* and robust H_∞ controllers are synthesized , taking into account the specific features of electro-hydraulic systems, and an adaptive intelligent control structure is proposed, providing automatic parameter tuning and improving the quality of regulation. A comparative analysis of classical and intelligent controllers is made, which proves the advantages of the proposed solutions in terms of speed, overregulation and resistance to disturbances.

Applied contributions

1. A hardware-software system for controlling an electrohydraulic tracking system (EHTS) has been developed , as well as a *MATLAB/Simulink* model, operating in real time, for studying the processes in the EHTS.

2. Models of loading subsystems, implemented through a proportional safety valve and an adjustable throttle, are proposed and analyzed , with an assessment of their impact on the dynamics of the system.

3. It has been experimentally proven that the dynamic characteristics of the system can be improved when using intelligent controllers, resulting in reduced overshoot, shortened re-measurement of transients, and increased resistance to disturbances.

List of publications on the dissertation

1. Kostov K. , K. Ormandzhiev, S. Yordanov , G. Mihalev, K. Delchev, Stability region of an electrohydraulic tracking system with a rotary actuator, Mechanics of Machines, Year XXXIV, Book 1, 2026, pp. 107 – 111, ISSN 0861-9727.

2. Ormandzhiev K., S. Yordanov , G. Mihalev, **K. Kostov** , K. Delchev, Parametric identification of an electrohydraulic tracking system, Mechanics of Machines, Year XXXIV, Book 1, 2026, pp. 112 – 116, ISSN 0861-9727.

3. Kostov K., Experimental study of an electrohydraulic tracking system with a rotary actuator, STUDENT SCIENTIFIC SESSION'2024, Technical University - Gabrovo, Gabrovo, October 18, 2024.

4. Yordanov S., K. Ormandzhiev, G. Mihalev, **K. Kostov** and V. Mitev, Studying the influence of working fluid temperature on the performance of an electrohydraulic servo system in dynamic mode, International Conference AUTOMATICS AND INFORMATICS`2023 (ICAI'23), Varna, Bulgaria, October 05 - 07, 2023

5. Mihalev G., S. Yordanov, K. Ormandzhiev, **K. Kostov** , V. Mitev, Robust Control of Electro-Hydraulic Servo System, International Conference Automatics and Informatics, ICAI 2022, 06-08 October, 2022, IEEE, Varna, Bulgaria, DOI: 10.1109/ICAI55857.2022.9960130

6. Yordanov S., Ormandzhiev K., Mihalev G., **Kostov** K. Identification and synthesis of PI controller for electrohydraulic servo system. 2020 International Conference Automatics and Informatics, ICAI 2020 - Proceedings , 1-3 October 2020, Varna, Article number 9311366, pp. 1-4, ISBN 978-172819308-3

7. Ormandzhiev K., Yordanov S., Mihalev G., **Kostov** K. Parametric Optimization of Electrohydraulic Servo System. 25th Scientific Conference on Power Engineering and Power Machines (PEPM'2020), E3S Web of Conferences, Vol. 207, 2020, Article Number 04003pp. 1-10, ISSN 2267-1242 (**SJR 0.203**)